PNNL-13588

Pacific Northwest
National Laboratory
Operated by Battelle for the
U.S. Department of Energy

# Sulfur Partitioning During Vitrification of INEEL Sodium Bearing Waste: Status Report

J. G. Darab
D. D. Graham
B. D. MacIssac
R. L. Russell
H. D. Smith
J. D. Vienna
Pacific Northwest National Laboratory, Richland, WA 99352

D. K. Peeler
Westinghouse Savannah River Company, Aiken, SC 29808

March 2001

Prepared for the U.S. Department of Energy
under Contract DE-AC06-76RL01830

PACIFIC NORTHWEST NATIONAL LABORATORY
*operated by*
BATTELLE MEMORIAL INSTITUTE
*for the*
UNITED STATES DEPARTMENT OF ENERGY
*under Contract DE-AC06-76RLO 1830*

PNNL-13588

# Sulfur Partitioning During Vitrification of INEEL Sodium Bearing Waste: Status Report

J. G. Darab, D. D. Graham, B. D. MacIssac, R. L. Russell,
H. D. Smith, and J. D. Vienna

*Pacific Northwest National Laboratory, Richland, WA 99352*

D. K. Peeler

*Westinghouse Savannah River Company, Aiken, SC 29808*

July 2001

Prepared for the U.S. Department of Energy
under Contract DE-AC06-76RLO 1830

Pacific Northwest National Laboratory

Richland, Washington 99352

# Summary

The loading of Idaho National Engineering and Environmental Laboratory sodium bearing waste (SBW) in glass will be limited by the allowable concentration of sulfate in the feed which is defined by the highest concentration that can be vitrified into glass at an acceptable rate without the accumulation of molten salt on the melt surface. This allowable concentration of sulfate in the feed is determined by many chemical (e.g., waste composition, chemistry of glass forming additives, waste loading, acid or reductant addition) and physical (e.g., melter-feed rate, plenum temperature, heat-transfer rate to the cold cap) parameters. This report documents the status of an ongoing study to determine the impacts of key processing parameters on the partitioning of sulfur species between the glass, a molten salt phase, and the off gas. As this study is continuing, the nature of these results is preliminary and incomplete. However, this report does give an indication of the relative importance of many parameters and the range of expected sulfur-partition coefficients during SBW vitrification.

A series of tests was conducted to measure the partitioning of sulfur species between glass, the off gas, and a molten salt. In crucible tests, between 79 and 100% of the total sulfur was found to remain in the glass, and molten salts were not formed until the target concentration of sulfur in the glass exceeded roughly 1 mass% on an $SO_3$ basis. The use of high gas purge rates (e.g., 2300 ccm) in crucible tests decreased the fraction of sulfur in the glass to roughly 23% of that targeted. The influence of sugar concentration, heating rate, and starting feed pH were found to be minimal on the partitioning of sulfur species in these tests. Glass-forming additive composition was found to influence the formation of a salt layer. Details of the crucible tests are reported by Peeler et al. (2001).

Three melter tests were performed with simulated SBW feed. The first test (EV-16-1999-1) was performed using the pilot-scale Envitco EV-16 melter at Clemson University in April 1999. The as-batched glass composition for this test contained 1.07 mass% of $SO_3$. The measured concentration of sulfur in the glass produced was roughly 0.58 mass% based on $SO_3$. No salt layer was observed during or after the test, suggesting that the remaining sulfur was driven to the off gas. However, power excursions occurred during the test, which occasionally brought the melt temperature to 1350°C. These excursions may have had a strong influence on the partitioning of sulfur during the test. Results of this test have yet to be published; highlights are described in Section 3.1.

The second melter test (RSM-01-1) with simulated SBW feed was performed using the Research-Scale Melter (RSM) at Pacific Northwest National Laboratory in January 2001. This test was conducted in eight segments. The waste loading (30 to 35 mass% on a dry, non-volatile oxide basis), sulfur concentration (1.07 to 1.75 mass% based on $SO_3$), and sugar concentration (135 to 197 g/L of waste simulant) were varied. A salt accumulation was observed with target sulfur concentrations in the glass of 1.25 mass% based on $SO_3$ (35% waste loading) and higher. Between 51 and 63% of the target amount of sulfur fed to the melter was found in the glass. Roughly, 25% of the target sulfur amount fed to the melter was captured in the off-gas system with roughly 80% of that coming from the high-efficiency mist eliminator (HEME). Since only a small fraction of the sulfur fed to the melter was found in the molten salt after the test, the remaining sulfur was likely partitioned to the off gas, but escaped analyses. Details of this test are described by Goles et al. (2001), with highlights discussed in Section 3.2.

A third melter test (EV-16-2001-1) was performed using the EV-16 melter at Clemson University. The target glass composition used in this test was the same as that fabricated during the first two segments of the RSM-01-1 test—30 mass% waste loading (on a dry, non-volatile oxide basis), SBW-9 additive mix (see Section 1.0). The concentration of sugar in the feed, however, was 160 g/L of waste simulant. The concentration of sulfur in the melter glass was found to be roughly 0.77 mass% on an $SO_3$ basis, which accounts for 72% of the total target sulfur fed to the melter. A salt layer formed during the test and was found to contain roughly 8% of the target sulfur fed to the melter. Although analyses of sulfur species in the off gas were not yet available at the time of this report, it is assumed that the remaining 20% of target sulfur fed to the melter partitioned to the off gas. Results from this test, which will be published in the near future, are summarized in Section 3.3.

An integrated feed-to-glass test method, called the Centimeter-Scale Melter (CSM), was designed to obtain sulfur partitioning values that closely match those of the larger, more expensive, melter tests. The CSM was used to measure the effects of a number of chemical and physical parameters on sulfur partitioning during SBW vitrification. It should be noted that effects of target glass compositions were not yet available at the time of this report. The concentration of sulfur in the glass ranged from 0.35 to 1.14 mass% on a $SO_3$ basis with the fraction of target sulfur fed to the CSM partitioning to the glass ranging from 31 to 100%, depending on the feed chemistry and processing parameters. The remaining fraction of sulfur partitioned primarily to the off gas where it was captured in a scrub solution. A small fraction of the sulfur partitioned to a molten salt during some tests. The fraction of sulfur to partition to the glass in CSM tests matched that of the EV-16-2001-1 test very closely, while the formation of a molten salt more closely matched that of the RSM-01-1 test. The CSM identified those parameters that most strongly affect the partitioning of sulfur and helped to interpret the differing results between the two recent melter tests. The feed rate and sulfate concentration in the feed were found to have the strongest influence on the amount of molten salt formed. Sugar concentration had the largest effect on the fraction of target sulfur that partitioned to the glass. The CSM results are discussed in Section 4.0 of this report.

Generally, during the vitrification of simulated SBW, sulfur partitions between the glass, off gas, and in some instances a molten salt phase. Based on the preliminary results discussed in this report, we expect the following:

- the accumulation of a molten salt layer can be avoided with control of certain chemical and physical parameters such as feed rate, sugar concentration, and sulfate concentration
- between 55 and 75% of the total sulfur fed into the melter is likely to partition to the glass
- the remaining sulfur is likely to be captured by wet scrubbing of the off gas or in the HEME.

However, these results are preliminary, and further testing is required to confirm them, to determine how to control the partitioning of sulfur, to understand the impacts of scale-up, and to optimize the vitrification process.

## References

Peeler, D. K., J. D. Vienna, T. B. Edwards, J. V. Crum, I.A. Reamer, M. J. Schweiger, and R. J. Workman, 2001. *Glass Formulation development for INEEL Sodium-Bearing Waste (WM-180)*, WSRC-TR-2001-00295, Rev. 0, Westinghouse Savannah River Company, Aiken, South Carolina.

Goles R. W., J. M. Perez, B. D. MacIsaac, D. D. Siemer, and J. A. McCray. 2001. *Testing Summary Report INEEL Sodium Bearing Waste Vitrification Demonstration RSM-01-1*, PNNL-13522, Pacific Northwest National Laboratory, Richland, Washington.

# Glossary

| | |
|---|---|
| AZS | alumina-zirconia-silica |
| CSM | centimeter-scale melter |
| DIW | deionized water |
| DOE | U.S. Department of Energy |
| DTA | differential thermal analysis |
| GC | gas chromatograph |
| HEME | high-efficiency mist eliminator |
| HLW | high-level waste |
| ICP | inductively coupled plasma |
| ICPP | Idaho Chemical Processing Plant |
| INEEL | Idaho National Engineering and Environmental Laboratory |
| INTEC | Idaho Nuclear Technology and Engineering Center |
| LAW | low-activity waste |
| MS | mass spectrometer |
| OES | optical emission spectrometry |
| OX | oxidizing |
| PNNL | Pacific Northwest National Laboratory |
| PUREX | plutonium-uranium extraction |
| RED | reducing |
| RSM | Research-Scale Melter |
| SBW | sodium bearing waste |
| SLRD | slightly reducing |
| SRTC | Savannah River Technology Center |
| TFA | Tanks Focus Area |
| TGA | thermogravimeteric analysis |
| VRED | very reducing |
| WM | waste management |
| XRD | X-ray diffraction |
| XRF | X-ray fluorescence spectroscopy |

# Acknowledgments

The authors would like to acknowledge very useful conversations and suggestions from Pavel Hrma, Denny Bickford, Dong Kim, Darryl Siemer, and Ron Goles. We are indebted to Wayne Cosby for his artful editing of the manuscript and Keith Perry, John McCray, Dan Griffin, Dong Kim, and Loni Peurrung for review and comments to the report. We thank David Best, May Lin Thomas, and Ron Sanders for chemical analyses of samples, and Mike Schweiger, Jarrod Crum, and Irene Reamer for Laboratory assistance. Bill Holtzscheiter from the TFA and Chris Musick from the INEEL HLW program gave invaluable management support for this project. We would also like to thank Jerry Christian and Charles Barnes for waste and simulant compositions.

This study was funded by the Department of Energy's (DOE's) Office of Science and Technology, through the Tanks Focus Area, and Office of Waste Management through the Idaho National Environmental and Engineering Laboratory High-Level Waste Program. Pacific Northwest National Laboratory is operated for DOE by Battelle under Contract DE-AC06-76RL01830.

# Contents

# Figures



# Tables

# 1.0 Introduction

For about four decades, radioactive wastes have been collected and calcined from nuclear fuels reprocessing at the Idaho Nuclear Technology and Engineering Center (INTEC), formerly Idaho Chemical Processing Plant (ICPP). Over this time span, secondary radioactive wastes have also been collected and stored as liquid from decontamination, laboratory activities, and fuel-storage activities. These liquid wastes are collectively called sodium-bearing wastes (SBWs). About 3.8 million liters of these wastes are temporarily stored in stainless steel tanks at the Idaho National Engineering and Environmental Laboratory (INEEL). The Batt Settlement Agreement was established in August 1995 between the U.S. Navy, the U.S. Department of Energy (DOE), and the State of Idaho (DOE 1995). One of the requirements per this agreement is to remove SBW from the storage tanks by the end of 2012. More immediately, testing must be performed to provide information required to initiate the design of the SBW treatment facility in year 2002. Hence, direct vitrification (no or minimal feed conditioning before vitrification), which is being considered as an immobilization step for SBW, is the focus of this report. The DOE Office of Science and Technology (through the Tanks Focus Area [TFA]) and the Office of Waste Management (through the INEEL High-Level Waste [HLW] Program) are sponsoring a joint effort by INEEL, the Pacific Northwest National Laboratory (PNNL), and the Savannah River Technology Center (SRTC) to investigate processes and formulations for immobilizing INTEC HLW. This report documents the status of a joint study on the fate of sulfur species during SBW vitrification.

Sodium bearing waste is an acid solution with relatively high concentrations of $NO_3^{2-}$, $Na^+$, $Al^+$, $K^+$, and $SO_4^{2-}$. An initial glass formulation for the direct vitrification of an SBW (SBW-1) was developed by Vienna et al. (1999). It was determined that the presence of sulfur species, hereafter often referred to simply as "S," in SBW would ultimately limit the loading of SBW in glass. The allowable concentration of S in the feed is the highest concentration that can be processed at an acceptable rate without accumulating a molten salt on the melt surface. This allowable concentration of S in the feed is determined by many chemical (e.g., waste composition, chemistry of glass forming additives, waste loading, acid or reductant addition) and physical (e.g., melter feed rate, plenum temperature, heat-transfer rate to the cold cap, sweep-gas flow rate) parameters.

The direct vitrification of SBW was first demonstrated in an Envitco EV-16 pilot-scale melter at Clemson University with the glass composition developed by Vienna et al. (1999). Further glass-composition development for SBW immobilization was conducted by Peeler et al. (2001) on subsequent composition estimates of SBW based on a measurement of the INTEC waste tank WM-180. The composition of the SBW frits and waste simulants are listed in Table 1.1 through Table 1.3. A Research Scale Melter (RSM) test was conducted using the WM-180 simulant with the SBW-9 glass composition developed by Peeler et al. (2001) (Goles et al. 2001). This was followed by a pilot-scale melter demonstration in the Envitco EV-16. The results of these tests confirmed that the loading of SBW in glass will be limited by the maximum allowable concentration of S in the feed without the accumulation of a molten salt phase**.** Similar behavior has been described by Pegg et al. (2001) with selected Hanford low-activity waste (LAW) streams. Thus, an understanding of how S partitions between the glass, salt layer, and off gas is critical to developing glass compositions and process chemistries for the vitrification of SBW.

**Table 1.1. Frit (or additive mix) Compositions Used in Recent SBW Vitrification Tests (in mass% of non-volatile oxides)**

| Oxide | SBW-1 | SBW-2 | SBW-3 | SBW-4 | SBW-5 | SBW-6 | SBW-7 | SBW-8 | SBW-9 | SBW-10 |
|---|---|---|---|---|---|---|---|---|---|---|
| $SiO_2$ | 68.69 | 69.61 | 66.11 | 70.00 | 65.00 | 67.00 | 66.00 | 63.00 | 65.00 | 70.00 |
| $B_2O_3$ | 14.26 | 12.00 | 15.00 | 12.00 | 15.00 | 15.00 | 10.00 | 15.00 | 15.00 | 12.00 |
| $Li_2O$ | 2.67 | 4.00 | 4.50 | 4.00 | 4.00 | 4.00 | 5.00 | 5.00 | 5.00 | 4.00 |
| $Fe_2O_3$ | 11.31 | 11.31 | 11.31 | 12.00 | 12.00 | 12.00 | 15.00 | 15.00 | 10.00 | 12.00 |
| $TiO_2$ | 3.08 | 3.08 | 3.08 | 0.00 | 0.00 | 0.00 | 0.00 | 0.00 | 0.00 | 0.00 |
| CaO | 0.00 | 0.00 | 0.00 | 2.00 | 4.00 | 2.00 | 4.00 | 2.00 | 5.00 | 0.00 |
| BaO | 0.00 | 0.00 | 0.00 | 0.00 | 0.00 | 0.00 | 0.00 | 0.00 | 0.00 | 2.00 |

**Table 1.2. Waste Simulant Compositions Used in Recent SBW Vitrification Tests (in mass% of non-volatile oxides)**

| Oxide | 1998 SBW | 2000 WM-180 | Oxide | 1998 SBW, cont'd | 2000 WM-180, cont'd | Oxide | 1998 SBW, cont'd | 2000 WM-180, cont'd |
|---|---|---|---|---|---|---|---|---|
| $Al_2O_3$ | 27.34 | 27.96 | F | 0.98 | 0.57 | NiO | 0.55 | 0.09 |
| $B_2O_3$ | 0.65 | 0.35 | $Fe_2O_3$ | 1.55 | 1.43 | $P_2O_5$ | 1.19 | 0.80 |
| BaO | 0.00 | 0.01 | $Gd_2O_3$ | 0.00 | 0.03 | PbO | 0.31 | 0.24 |
| CaO | 2.23 | 2.22 | I | 0.02 | 0.01 | $RuO_2$ | 0.04 | 0.01 |
| CdO | 0.00 | 0.08 | $K_2O$ | 7.92 | 7.62 | $SO_3$ | 3.73 | 3.57 |
| $Ce_2O_3$ | 0.00 | 0.01 | $Li_2O$ | 0.00 | 0.00 | $SiO_2$ | 0.18 | 0.00 |
| Cl | 1.04 | 0.88 | MgO | 0.05 | 0.40 | SnO | 0.02 | 0.00 |
| CoO | 0.00 | 0.19 | MnO | 0.78 | 0.82 | SrO | 0.00 | 0.01 |
| $Cr_2O_3$ | 0.25 | 0.00 | $MoO_3$ | 0.13 | 0.02 | ZnO | 0.00 | 0.07 |
| CuO | 0.00 | 0.05 | $Na_2O$ | 50.05 | 52.54 | $ZrO_2$ | 1.00 | 0.01 |

**Table 1.3. Key Ion Concentrations Used in Recent SBW Vitrification Tests (in moles/liter of waste)**

| Species | 1998 SBW | 2000 WM-180 |
|---|---|---|
| $[H^+]$ | 1.94 | 1.08 |
| $[NO_3^{2-}]$ | 6.96 | 5.11 |

In evaluating how S partitions during the vitrification of SBW on a laboratory scale, the simulated feed composition and manner of feed melting become important considerations that dictate the chemistry, thermodynamics, and kinetics of the process. A variety of feeds can be used to target a desired glass composition, e.g., 1) a dry mixture of oxides, carbonates and appropriate other salts, 2) a slurry of aqueous waste species (which usually include nitrates as well as added reductants such as sugar) along with glass forming compounds, or 3) a dried version of the aqueous-based feed.

Reductants such a sugar, glycolic acid, starch, graphite, and related sources of carbon will be added to the SBW. One action of these reductants will be to react with nitrate as the feed is heated and dried out in

an attempt to improve the melting rate of the feed. To illustrate, one of the possible reactions for carbohydrate with nitrates (e.g., $NaNO_3$) proceeds as follows:

$$5C_nH_{2n}O_n + 4nNaNO_3 \longleftrightarrow (2n)N_2\uparrow + (3n)CO_2\uparrow + (5n)H_2O\uparrow + (2n)Na_2CO_3 \quad (1.1)$$

The following reaction could also occur and is indicated by the generation of CO gas:

$$C_nH_{2n}O_n + 0.67nNaNO_3 \longleftrightarrow (0.33n)N_2\uparrow + (0.67n)CO_2\uparrow + (0.92n)H_2O\uparrow + (0.5n)Na_2O + (0.33n)CO\uparrow \quad (1.2)$$

For elemental carbon, the reaction would be written as the following:

$$3C + 2NaNO_3 \longleftrightarrow N_2\uparrow + 2CO_2\uparrow + CO\uparrow + Na_2O \quad (1.3)$$

The above reactions can also be written to include NO, $NO_2$, and $N_2O$ (and even $NH_3$), all of which are typically observed. For example, in the case of elemental carbon:

$$9C + 7.83NaNO_3 \longleftrightarrow N_2\uparrow + 3.3NO\uparrow + 1.25N_2O\uparrow + 6CO_2\uparrow + 3CO\uparrow + 3.92Na_2O \quad (1.4)$$

Mathematically, the molar ratios of all of these gases can be varied to give a range of possible reaction equations. Indeed, experimentally it is observed that a wide range of reaction-gas ratios occurs. Generally, the greater the carbon to nitrate ratio, the more reduced the average gas product is and vice versa.

The acidic SBW waste is similar to the plutonium-uranium extraction (PUREX) acid waste[(a)] that Bray (1963) denitrated with sucrose under conditions that match the heat up and boiling stages of the dry-out tests performed in this study. He found that the sugar-nitrate reaction began to react noticeably at approximately 85°C versus 80°C in the SBW system. Bray's tests were typically run in the temperature range of 95°C to 105°C, and he observed complete conversion of the carbohydrate to carbon dioxide. The oxidation sequence of the sugar molecule consists of two hydrolysis steps and three oxidation steps per molecule of carbon dioxide produced. Basically, the carbon–oxygen ring structure is opened, exposing the ends of the carbon backbone, and the oxidation proceeds carbon by carbon down the chain until no organic remains (excess nitrate) or various hydrocarbons remain (excess sugar). Bray's report (1963) gives the details of this reaction sequence. It was found that iron in the waste solution significantly increases the amount of nitrate destroyed per mole of sucrose from 12 moles of nitrate with 0.0 moles of $Fe^{3+}$ present to 20 moles of nitrate with 1.0 moles of $Fe^{3+}$ present. From this observation, it can be concluded that the following reactions occur and that $Fe^{3+}$ acts as a catalyst for the formation of NO:

when $M_{Fe} = 0.0$,

$$C^0 \text{ (hydrocarbon)} + N^{5+} \text{ (nitrate)} \longleftrightarrow C^{4+} \text{ (as } CO_2\text{)} + N^{+} \text{ (as } N_2O\text{)} \quad (1.5)$$

[(a)] The PUREX waste that Bray (1963) studied consisted of 4–8 M $H^+$, 5–7 M $NO_3^-$, 0.5–1.0 M $Fe^{3+}$, 0.7 M $SO_4^{2-}$, 0.7 M $Na^+$, 0.2 M $Ni^{2+}$, 0.1 M $Al^{3+}$, 0.1 M $Cr^{3+}$, 0.01 M $PO_4^{3-}$, and trace fission products.

and, when $M_{Fe} = 1.0$,

$$C^0 \text{ (hydrocarbon)} + N^{+5} \text{ (nitrate)} \longleftrightarrow 3C^{+4} \text{ (as } CO_2\text{)} + 5N^{2+} \text{ (as NO).} \quad (1.6)$$

Our results for Bray's temperature range appear to be a combination of the two reactions above.

The reactions that occur between the added reductants, nitrates, and perhaps other species in the waste often do not go to completion. In other words, residual nitrates, reductants, and other species that were targeted for mitigation may still be present in the resulting feed after dry out. Residual $NaNO_3$, for example, is capable of reacting with other components in the waste. Abe et al. (1983) have studied these reactions with $NaNO_2$ and $NaNO_3$ in detail. In the presence of $SiO_2$, $NaNO_3$ will react above ≈700°C to form $Na_2O$, $Na_2O_2$, and NO gas under non-oxidizing conditions. At higher temperatures, sodium silicate species and $O_2$ gas are formed.

Darab et al. (1999) observed such reactions during the vitrification of dried Hanford LAW simulant. They also observed that batch volume expansion begins to occur at approximately the same temperature at which the maximum $O_2$ off gassing occurs. These results are consistent in that a high rate of $O_2$ evolution represents a high degree of lower-melting sodium silicate formation with a corresponding loss of open porosity. The closing off of porosity inhibits off gas removal, thus altering the mechanisms through which volatile species can escape. Thus, compared to feeds prepared from oxides, carbonates, etc., the presence of nitrates in a dried slurry feed often significantly alters the reaction pathways as well as the off gas, redox, and melt chemistries associated with the vitrification process. These differences in chemistry can produce large differences in, for example, volatility (Darab and Smith 1996).

Further consider the differences between using an aqueous feed simulant or a dried version of the simulant. Although these feeds differ in water content and physical state, they should yield a glass with identical composition. When the aqueous slurry feed is rapidly heated, as would be the case if it were pumped into an operating melter at melt temperature, the vaporization of water and off gas generated from chemical reactions can cause components in the feed to be entrained with these gaseous species. The violent nature of these reactions can also eject feed into the atmosphere above the melt (i.e., atomizing it in a similar manner that spray dryers atomize salt solutions to form very fine particles). Such events could significantly alter the partitioning of species between the glass, salt layer, and off gas.

As this report will demonstrate, when laboratory-scale studies are to be used to help develop an envelope for the larger scale vitrification of waste, not only is it important to simulate the chemistry properly, but methods to more accurately simulate the process itself are needed. Of further concern for the work presented here is how S in SBW partitions during the vitrification process.

In SBW, as is typical for this and other (e.g., Hanford LAW) aqueous waste streams, S is present in the waste in the +6 oxidation state as $SO_4^{2-}$. As the waste is heated, either during a deliberate initial drying step or during the initial stages of liquid feed-to-glass conversion process, one might speculate that S is lost from the feed as $H_2SO_4$, either through direct volatilization or as entrained species in water vapor. The formation of $SO_3$, another S(VI) species, from $SO_4^{2-}$ is not very conceivable, since the strong reactivity of $SO_3$(g) with water to form $H_2SO_4$ suggests that the equilibrium for that reaction would strongly favor $SO_4^{2-}$ (Cotton and Wilkinson 1980a, pp. 529-533).

The presence of reductants, such as sugar, in the waste might also give rise to reduced aqueous S species (see below) or reduced gaseous S species, primarily $SO_2$. The fate of $SO_2$ (g) under the reaction conditions that will be described below is uncertain. $SO_2$ is reported to react with aqueous $Na_2CO_3$ (another potential component of certain complex aqueous waste streams) to form various S(IV) species: $NaHSO_3$ or $Na_2SO_3$, depending on the solution pH, and even $Na_2S_2O_5$ (Cotton and Wilkinson 1980a, pp. 529-533). Aqueous $SO_3^{2-}$, for example, can form $S_2O_3^{2-}$ in the presence of a reductant, form $SO_4^{2-}$ in the presence of species such as aqueous $Fe^{3+}$ (another component in SBW or a properly simulated feed), or revert back to $SO_2$ (Cotton and Wilkinson 1980a, pp. 529-533). In the presence of catalysts such as $V_2O_5$, Pt, and even NO, gaseous $SO_2$ reacts with oxygen to form $SO_3$, whose reactivity we have already discussed above (Cotton and Wilkinson 1980b, p. 245).

Reduced aqueous S species such as $HSO_3^-$ and $S_2O_3^{2-}$ are much more soluble on an S basis than, for example, $SO_4^{2-}$ (see Table 1.4), and thus provide a means by which S remains in solution longer. Longer solution residence times would thus allow for solution-based S-loss mechanisms (e.g., gaseous $H_2SO_4$ or $SO_2$ generation, entrainment of S species in water vapor, atomization of feed, etc.) to be active longer and may thus influence the partitioning of S in the final product.

**Table 1.4. Aqueous Solubility Limits of Sodium Salts of S at Different Solution Temperatures (in grams of S per 100 $cm^3$) (values were converted from grams of compound per 100 $cm^3$ reported in the CRC Handbook of Chemistry and Physics)**

| | Temperature, °C | | | |
|---|---|---|---|---|
| **Compound** | **0** | **20** | **80** | **100** |
| $Na_2SO_4$ | 1.07 | | | 9.63 |
| $Na_2S_2O_5$ | | 17.9 | | 27.5 |
| $Na_2SO_3$ | 3.185 | | 7.2 | |
| $NaHSO_3$ | vs | vs | vs | vs |
| $Na_2S_2O_3$ | | | | 93.6 |
| vs--indicated that the salt is qualitatively very soluble | | | | |

Although the above discussion focuses on the loss of S during the heating of SBW, a considerable amount of S will remain in the melter feed up to glass-melt temperatures. Considering the composition of SBW, ideally, one might then expect salts such as $Na_2SO_4$ and $CaSO_4$ (or perhaps reduced forms of these salts, e.g., $Na_2S_2O_3$, which may eventually re-oxidize under melt conditions) to form as the melter feed is dried at elevated temperatures. At melt temperatures of around 1150°C, these salts may contribute to the formation and/or accumulation of a molten salt layer on the melt surface. In laboratory-scale work, the importance of not only the chemical make-up but also the physical nature of the simulant formulations and the experimental methods will influence how these salts may assist in the formation of molten salt layers during SBW vitrification.

# 2.0 Segmented Feed-to-Glass Studies

## 2.1 Background

One approach to studying the vitrification of complex aqueous slurry-based wastes such as SBW is to use a chemically accurate simulant (removing radionuclides and other hazardous components), but break down the various vitrification regimes into segments: 1) aqueous and hydrothermal (i.e., hot water) reactions, 2) feed dry out, 3) dried feed-to-melt reactions, and 4) melt reactions. Although this does not precisely emulate the manner in which real waste will be vitrified, it is a reasonable compromise, allowing us to obtain pertinent information about each segment of the vitrification process. The information obtained using this segmented approach may allow for a qualitative link to feed behavior during melter processing.

## 2.2 SBW Simulant Preparation

Ten liters of SBW simulant (based on the 2000 WM-180 composition) were prepared for laboratory testing. Table 2.1 lists the chemicals used to make the simulant along with the amount of each. The simulant was prepared by mixing the dry salts in a beaker. Then enough deionized water (DIW) was added to dissolve all of the salts with heating and stirring. To this solution, the manganese nitrate solution and the aluminum nitrate solution were added. The resulting solution was continually heated and stirred as the boric acid was added to the solution. At this point, the heating and stirring were discontinued, and the solution was transferred to a plastic carboy. The hydrofluoric acid was then added to the solution and stirred. Then the sulfuric acid was added to the solution while stirring the solution vigorously. About 500 mL of DIW was added to the solution and then the hydrochloric, phosphoric, nitric, and molybdic acids were added to the solution. Finally, DIW was added to bring the final volume of the solution to 10 L. The resulting solution was then thoroughly mixed by stirring.

**Table 2.1. Chemicals Used in the Preparation of SBW Simulant**

| Chemical Used | Amount (g) | Chemical Used | Amount (g) | Chemical Used | Amount |
|---|---|---|---|---|---|
| $NaNO_3$ | 1650.60 | $Co(NO_3)_2\ 6H_2O$ | 0.05 | KI | 0.21 g |
| $KNO_3$ | 187.22 | $Cu(NO_3)_2\ 3H_2O$ | 1.59 | $Mn(NO_3)_2$ (50% soln) | 47.64 g |
| $Ca(NO_3)_2\ 4H_2O$ | 106.95 | $Gd(NO_3)_3\ 5H_2O$ | 0.73 | 2.2M $Al(NO_3)_3$ soln | 2855 mL |
| $Cd(NO_3)_2\ 4H_2O$ | 2.20 | $Pb(NO_3)_2$ | 4.08 | $H_3BO_3$ | 7.18 g |
| $Ni(NO_3)_2\ 6H_2O$ | 4.04 | $LiNO_3$ | 0.22 | 28.9M HF | 13.69 g |
| $Fe(NO_3)_3\ 9H_2O$ | 82.83 | $Mg(NO_3)_2\ 6H_2O$ | 29.13 | 18M $H_2SO_4$ | 52.07 g |
| $ZrF_4$ | 0.10 | $RuCl_3$ | 0.24 | 12M HCl | 27.38 g |
| $Cr(NO_3)_3\ 9H_2O$ | 12.66 | $Sr(NO_3)_2$ | 0.24 | 14.6M $H_3PO_4$ | 15.13 g |
| $Ba(NO_3)_2$ | 0.14 | $TiO_2$ | 0.04 | 15.4M $HNO_3$ | 804.4 g |
| $Ce(NO_3)_3\ 6H_2O$ | 0.19 | $Zn(NO_3)_2\ 6H_2O$ | 2.95 | $H_2MoO_4$ | 0.295 g |

## 2.3 Aqueous and Feed Dry-out Reactions

Three feed-drying tests were performed to characterize the gas evolution, determine the amount of S partitioning to the off gas during drying, and observe the melter-feed characteristics during the drying process. Melter feed was prepared using the 2000 WM-180 composition (see Table 1.2), silica, boric acid, iron oxide, calcium hydroxide, and lithium hydroxide. About 200 mL of melter feed was placed in a sealed reaction vessel as shown in Figure 2.1. The sealed reaction vessel was placed on a hot plate and heated to boiling. The condensate was removed, and the melter feed was allowed to boil to dryness. The temperature of the dried melter feed was further increased to at least 250°C. Off-gas measurements were taken continuously throughout the tests using an MTI-100 gas chromatograph (GC), a Rosemont $NO_x$ analyzer, and a quadrapole mass spectrometer (MS). However, the GC was not used during the first dry-out test. The GC measured for $H_2$, He, $O_2$, $N_2$, CO, $CO_2$, and $N_2O$. The $NO_x$ analyzer monitored for NO and $NO_2$. During these tests, the $NO_2$ converter was not working, so only NO was measured. However, there are several reasons to expect the ratio of NO to $NO_2$ to strongly favor NO. Only NO was expected to predominate from the batch reactions, based on previous studies (Smith et al. 1995; Smith et al. 1999; Darab et al. 1999, for example). $NO_2$ would result from the oxidation of the NO in the off gas after leaving the batch blanket. The extent of reaction of NO oxidation to $NO_2$ would also be expected to be quite low. The MS monitored for $SO_2$ and $SO_3$ in the second and third tests.

**Figure 2.1. Photograph of Dry-Out Test Reaction Vessel**

Dry out test #1 was performed with feed with a target composition of SBW-4 additive mix, 35 mass% of 2000 WM-180 waste (on a dry non-volatile oxide basis), and 141 g sugar per liter of waste simulant. This test was originally designed as a test to detect potential reactions between the sucrose and nitrate under ambient conditions. The system consisted of a 2-L reaction vessel containing the simulated melter feed with a Teflon-coated magnetic stir bar placed on a hot plate with magnetic stirring capabilities

without any heating. The vessel was continually purged at 1.95 L per minute with argon gas containing about 500 ppm helium. No nitrogen oxides were detected after running the test for several days under ambient conditions and analyzing the purge gas exiting the reaction vessel. The slurry was then heated to boiling on the hot plate while analyzing the purge gas for reaction products, such as nitrogen oxides, that were expected from the reduction of nitrate by sucrose. The test was performed by turning the hot plate on to maximum power while stirring rapidly enough to maintain a visually homogeneous slurry. A thermocouple was positioned in the stirring slurry near the bottom of the slurry pool and away from the magnetic stir bar. Stirring was continued during the boil down of the slurry until the slurry had thickened, and stirring was no longer possible. It was necessary to stop the heating and open the system to remove the stir bar. The temperature profile in Figure 2.2 indicates the period when heating was discontinued to retrieve the stir bar. Following the concentration stage of the test, the hot plate was maintained at full power until the temperature rose to the maximum level that could be generated with the system or the off-gas generation dropped to relatively low levels, indicating that these reactions were essentially complete. For dry-out test #1, completion of the test was indicated by a strong exotherm followed by a precipitous drop in off-gas production while the system temperature was still elevated. Note that during this test, other potential reaction gases such as nitrogen, nitrous oxide, or carbon dioxide were not measured.

Dry-out test #2 was run essentially the same as dry-out test #1, except a GC (MTI-100) was used to make it possible to detect and measure all of the expected reaction gases in both the concentration and subsequent heating portions of the test. A mechanical, stainless steel stir shaft was used instead of a magnetic stir bar to keep the slurry thoroughly mixed. Chemically, dry-out test #2 differed from dry-out test #1 with respect to the amount of $HNO_3$ present in the melter feed, which was available to react with the sucrose. To the SBW simulant, sufficient $HNO_3$ was added to bring the $H^+$ concentration to 3.0 M.

Dry out test #3 was performed with feed with a target composition of SBW-9 additive mix, 32 mass% of 2000 WM-180 waste (on a dry non-volatile oxide basis), and 135 g sugar per liter of waste simulant. This test was run essentially the same as dry-out test #2, with the GC and MS off-gas analyses and stainless steel stir shaft. During the test, a pressure excursion caused the reaction vessel to break. The time of the break (approximately 69 min) can be seen in the off-gas trace in Figure 2.4.

Figure 2.2 through Figure 2.4 show the off-gas profiles for each of the dry-out tests. During the melter feed dry-out tests, the feed temperature rose from ambient to the boiling point of the supernatant of the melter feed slurry. After reaching the boiling point, the temperature of the drying system was controlled by the boiling point of the supernatant (101°C) until the amount of supernatant remaining was too small to maintain a liquid slurry. The temperature rise, after this stage of drying was reached, was controlled by the rate of heat transfer into the system minus the rate of heat transfer out of the system modified by any exothermic or endothermic reactions occurring in the system.

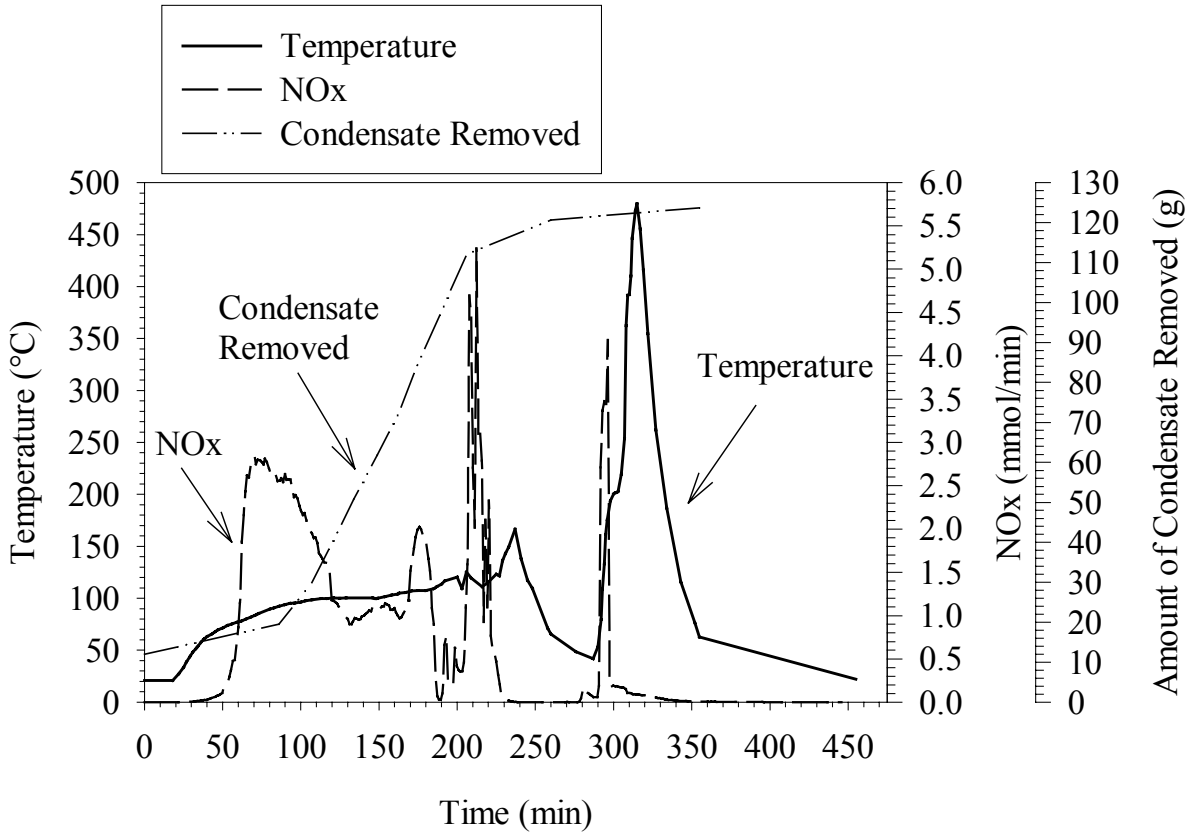


**Figure 2.2. Temperature, $NO_x$ Evolution, and Condensate Volume vs. Time for Dry-out Test #1**

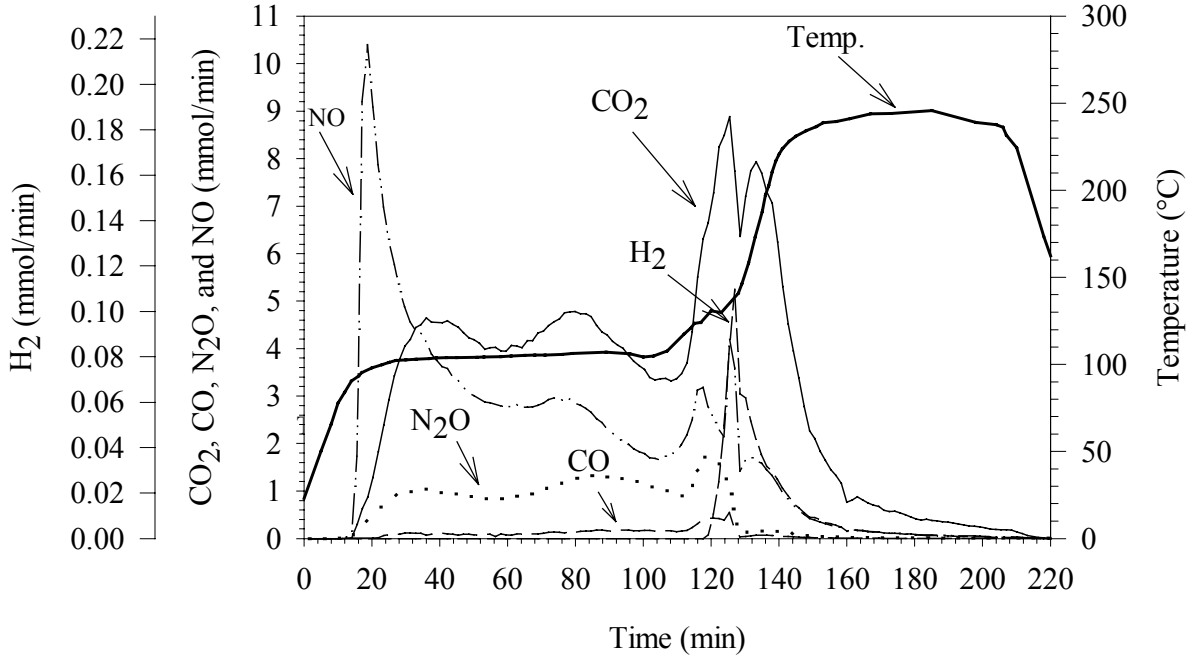


**Figure 2.3. Temperature and Off Gas Volume vs. Time (in minutes) for Dry-out Test #2**

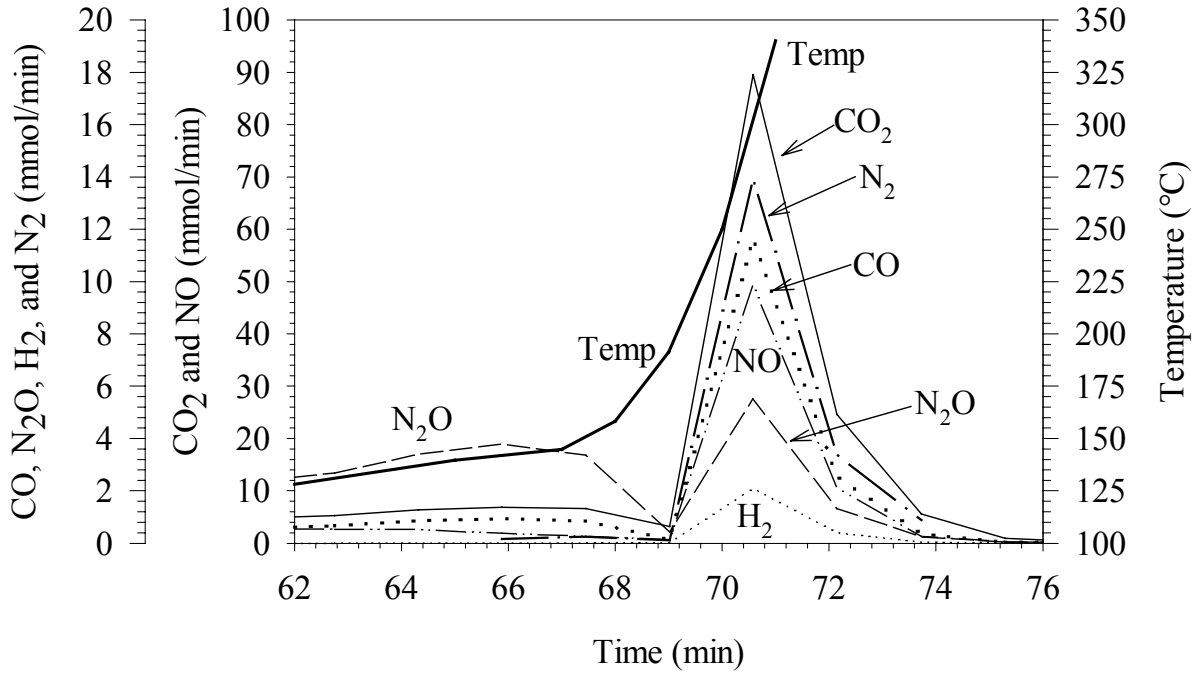


**Figure 2.4. Temperature and Off Gas Volumes vs. Time for Dry-out Test #3 (note that the reaction vessel broke at roughly 69 min)**

As the melter feed was heated to boiling, reactions between these simple sugars and nitrate began at approximately 80°C based on the initiation of NO production in dry-out test #1 (again the GC was not used in this test) and $N_2O$, NO, CO, and $CO_2$ production in dry-out test #2. The rate of reaction increased with temperature to boiling conditions as shown in Figure 2.2 through Figure 2.4. During the final stages of the first dry-out test, after the melter feed was dry and when the temperature was increasing, a strong exothermic reaction was observed that caused the temperature to spike to about 450°C accompanied by a burst of NO emission. The thermocouple temperature was at approximately 220°C when this exotherm began. However, the thermocouple location in the dried melter feed was not right at the bottom of the reaction vessel, so this temperature may not correspond to the temperature where the reaction initiated. The conclusion is that a direct reaction between nitrate and sugar occurred at this stage, indicating that both nitrate and sugar were still present in the test materials. This is a well-documented reaction between nitrate and sugar under anhydrous conditions that initiates at about 260°C (Smith et al. 1999). On the other hand, in dry-out test #2, little if any exothermic activity was observed at this stage of the test. The off-gas profiles indicate a pulse of off-gas activity, but the peaks are broader, and no temperature spike was observed. The broader and muted peaks indicate that the energetic reaction that occurred in dry-out test #1 did not occur in dry-out test #2. The additional free acid present in dry-out test #2 is believed to have consumed much of the sugar during the boiling phase. (Note that since $CO_2$ was not measured for the first test, we cannot compare the tests on that basis.) However, when comparing the NO generation rate, the rate of NO evolution during the second test (more free acid) peaked at about twice the rate observed during the first dry-out test, indicating a greater rate of reaction. This results in a disproportionately larger amount of nitrate remaining, and this is thought to reduce the rate of the

anhydrous sugar-nitrate reaction. It also explains the lack of a pronounced temperature spike at this stage of the test (Beitel 1976).

During dry-out tests #2 and #3, no $SO_2$ or $SO_3$ were detected in the off gas at the sensitivity level of the MS. The total amount of S found in the condensate and off-gas plumbing corresponded to 2.1, 0.2, and 0.7 percent of the amount of S in the starting feeds of tests #1, #2, and #3, respectively. Analyses of the dried feeds suggested that within measurement uncertainty, 100% of the starting S remained in the dry feed. Based on these results, we conclude that less than 2.5% of the S is lost to the off gas during drying of the melter feed and that increasing the concentration of free acid from ~1 M to 3 M did not increase the amount of S liberated to the off gas.

## 2.4 Dried Feed-To-Melt Reactions

To assess the reactions occurring during the dried feed to melt segment, a series of analytical tools and techniques were used. Section 2.4.2 discusses the use of thermogravimeteric analysis/differential thermal analysis (TGA/DTA) on monitoring the reaction of the temperatures and gases evolved during the conversion of the SBW melter feed material to a glass product. The influence of batch expansion was studied using a quartz crucible furnace as discussed in Section 2.4.3. To identify the phases present at the different stages of the batch-to-glass conversion, X-ray diffraction (XRD) was used on quenched samples as discussed in Section 2.4.4. Section 2.4.5 discusses the results obtained from crucible melts with both a sweep gas and a static atmosphere (i.e., sealed crucibles with no sweep gas). Finally, thermodynamic calculations using FACT were performed to assess the potential for sulfur loss during melting.

### 2.4.1 Feed Preparation

Tests were performed with the SBW simulant prepared in a 10-L batch according to the batch composition listed in Table 2.1. The dry additives, required to form the final glass composition, were slowly mixed into the waste simulant either in a Teflon beaker with a Teflon-coated stir rod or directly in a 500-mL alumina melting crucible. Sugar was also added to this mixture (the amount of sugar was 141 g/L of SBW simulant in most tests with any differences being noted). In many cases, the total pH was adjusted by concentrated $HNO_3$ to determine the impacts of pH on sulfur partitioning. The mixtures were heated on a hot plate with continued stirring using a hot-plate face temperature of roughly 140°C until nearly dry (approaching a paste-like consistency). The mixtures were then transferred to drying ovens to dry overnight (approximately 16 h) at 100°C.

### 2.4.2 TGA/DTA/Evolved Gas Analysis

Using a TA Instruments 2960 TGA/DTA, simultaneous TGA and DTA were performed on the dried SBW-4 feed (35 mass% waste loading) to provide additional insight into the temperatures and gases evolved at each of the reactions during the conversion of the SBW melter feed material to a glass product. Samples were analyzed to temperatures greater than 1150°C at heating rates of 1, 5, and 25°C in an atmosphere of He/2%Ar. The TGA and DTA results as a function of temperature show the temperatures where major reactions occurred and the weight loss associated with each reaction.

The gas that evolved during the TGA/DTA run made at 5°C min was analyzed by gas chromatography-mass spectrometry (GC-MS) using a Hewlett Packard model 5890 GC and a model 5971 MS. The GC's Pora PLOT Q column was maintained at 90°C. The inlet pressure was 6.1 psig, and a corresponding backpressure regulator was set at 6.1 psig (to avoid baseline upsets). GC injections of 0.5 mL were made once a minute by a valve rotator. A sweep gas of 2% Ar in He was used at a flow rate of 50 mL/min. The gases that were monitored quantitatively included $O_2$, $CO_2$, CO, $SO_2$, NO, $N_2O$, and $CH_4$. The GC-MS results obtained from the SBW-4 feed (35 mass% waste loading) are summarized in Figure 2.5. No $SO_2$ was detected during the course of this run.[(b)] Due to the size of the sample (a few milligrams), the final glass was not chemically analyzed. Figure 2.6 compares the mass loss (determined by TGA) and total measured off-gas generation rates for the measurement as a function of temperature.

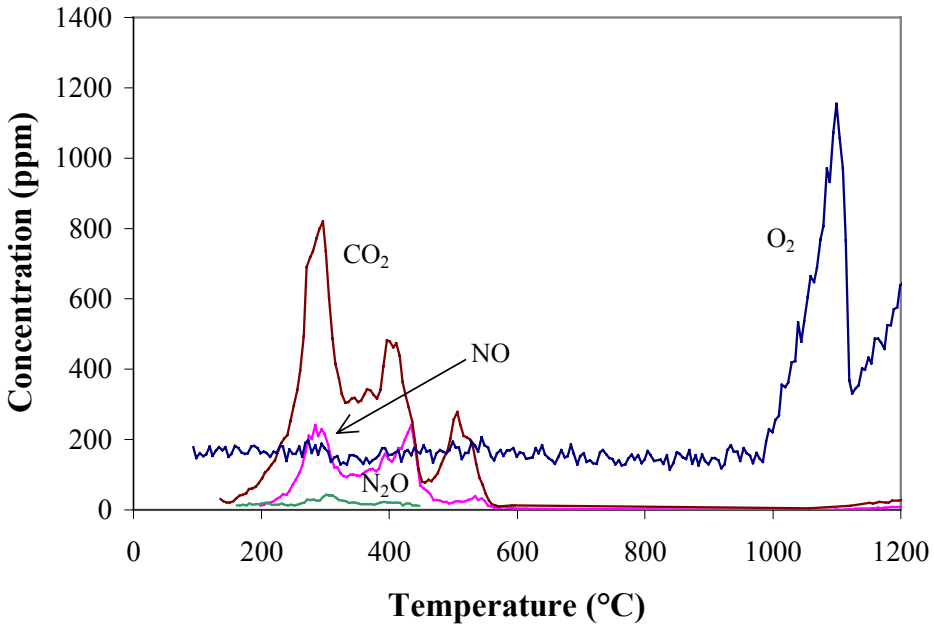


**Figure 2.5. SBW-4 Feed (35 mass% waste loading) Off-Gas Test Results**

(b) The fraction of total sulfur that must be evolved for $SO_2$ concentration to be above the GC-MS detection limit has not been fully determined; however, initial estimates indicate it to be a significant fraction (see Section 4.3).

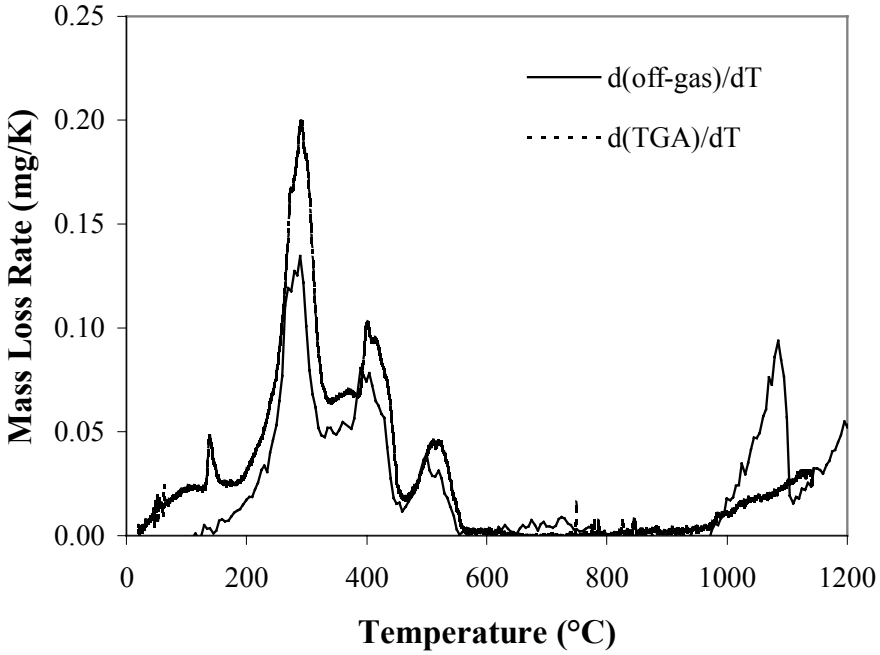


**Figure 2.6. Comparison of Off Gas and Mass Loss Rates for the SBW-4 Feed**

### 2.4.3 Quartz Crucible Experiment

Approximately 2.5 g of dried SBW-4 feed, with 35 mass% waste loading (on a dry, non-volatile oxide basis) and 141 g sugar per liter of waste simulant, were placed in a closed Quartz Crucible (QC) and heated to 1200°C at a rate of 5°C/min in a vertical tube furnace equipped with a viewing window. A sweep gas of 2 % Ar in He was used at a flow rate of 100 mL/min. The details of this experimental set up, which are discussed elsewhere (Smith et al. 1995), enable the reaction progress to be monitored *in situ* during heating. On a basic level, this quartz crucible setup may be considered similar to the crucible melt experiments performed with a sweep gas (see Section 2.4.5). However, the quartz crucible setup allows for greater flexibility and control of the sweep-gas composition and for the collection of off-gas species (if so desired). In the work presented here, we relied on off-gas collection from the TGA/DTA experiments as well as the centimeter-scale melter experiments (see Section 4). The quartz crucible setup also allows for unbridled batch expansion to occur—an event which, as discussed previously, may influence the loss of S species, but which needs to be constrained in traditional crucible melt studies (for example, by using variable heating rates and constant-temperature holds to allow particular reactions to go to completion). After the dried feed was heat treated and allowed to cool to room temperature, a sample of the resulting glass was broken from the crucible, ground in a tungsten-carbide mill, fused in $Na_2O_2$ and KOH, dissolved in $HNO_3$, and then analyzed by ICP-OES. Using this technique, the sample was determined to contain 0.320 mass% based on S. The target S content for this feed was 0.500 mass%, which means that 64% of the S in the feed was retained in the final glass after vitrification using this test method.

### 2.4.4 Ramp Heating and Selected Quenching Experiment

Separate portions of dried SBW-4 feed (35 mass% waste loading, 141 g sugar per liter of simulated waste) were ramp heated to several temperatures to determine the phase changes that corresponded to reactions observed with TGA/DTA (see Figure 2.6). Roughly 4-g to 5-g samples were heated at 5°C/min to 180, 350, 420, 465, 623, 701, 950, and 1150°C and then air quenched. The quenched samples were analyzed by XRD to identify the phases present at the different stages of the batch-to-glass conversion. The phases identified and their semi-quantitative concentrations are given in Table 2.2. Quartz ($SiO_2$), hematite ($Fe_2O_3$), and nitratine ($NaNO_3$) are identified in the dried feed, and their concentrations decrease with increasing temperature. As the nitratine decomposes to $Na_2O$, it reacts with quartz to form nepheline ($NaAlSi_2O_4$). The nepheline concentration increases with increasing temperature to 465°C, above which it decreases and totally dissolves between the temperatures of 701°C and 950°C. Nosean ($Na_8Al_6Si_6O_{24}[SO_4]$)[(c)] and $LiSiO_3$ are minor phases that were identified at higher temperatures of 701°C and 623°C, respectfully. $LiSiO_3$ dissolved between the temperatures of 701°C and 950°C. Nosean was the last crystalline phase to dissolve at temperatures between 950°C and 1150°C.[(d)] The lowest heating temperature at which an amorphous contribution to the XRD pattern of the quenched sample, presumably due to the presence of glass, could be resolved was 701°C. For the sample heated to 1150°C and quenched, only the presence of an amorphous phase could be identified by XRD.

**Table 2.2. Crystalline Phases Identified by XRD (in wt%) at Different Temperatures for SBW-4 Feed (35 wt% waste loading and 141 g/L of sugar). The percentage of mass with respect to the dried starting feed (100°C entry) during heating at each temperature is also indicated.**

| | Temperature, °C | | | | | | | | |
|---|---|---|---|---|---|---|---|---|---|
| **Phase** | **100** | **180** | **350** | **420** | **465** | **623** | **701** | **950** | **1150** |
| Quartz | 43.40 | 47.48 | 32.89 | 34.14 | 34.43 | 36.48 | 22.16 | 0.00 | 0.00 |
| Nepheline | 0.00 | 0.00 | 14.61 | 16.27 | 17.94 | 16.36 | 14.69 | 0.00 | 0.00 |
| Hematite | 4.41 | 4.90 | 4.07 | 4.43 | 5.12 | 4.26 | 2.58 | 0.00 | 0.00 |
| Nosean | 0.00 | 0.00 | 0.00 | 0.00 | 0.00 | 0.00 | 0.86 | 0.29 | 0.00 |
| $Li_2SiO_3$ | 0.00 | 0.00 | 0.00 | 0.00 | 0.00 | 1.64 | 0.52 | 0.00 | 0.00 |
| Nitratine | 16.71 | 15.41 | 0.00 | 0.00 | 0.00 | 0.00 | 0.00 | 0.00 | 0.00 |
| Total | 64.52 | 67.79 | 51.57 | 54.85 | 57.49 | 58.74 | 40.81 | 0.29 | 0.00 |
| Mass loss (%) | 0.0 | 0.8 | 38.5 | 38.7 | 38.6 | 39.8 | 41.3 | 41.7 | 41.7 |

(c) The XRD pattern fits best to $Na_8Al_6Si_6O_{24}[SO_4]$ (Nosean), although other anions, such as $Cl^-$, $OH^-$, and $PO_4^{3-}$, can substitute for the $SO_4^{2-}$ in Nosean. XRD may not be capable of distinguishing which analogue is actually present in the materials characterized here.

(d) A measurement of the liquidus temperature for this glass showed that no crystalline phases exist in equilibrium with the melt at temperatures above 1050°C (Peeler et al. 2001).

### 2.4.5 Crucible Melts

For SBW feed samples dried directly in alumina crucibles, lids were attached (see below), and the samples were melted directly in these same crucibles. For samples dried in Teflon beakers, the samples were first transferred to an alumina crucible, and the lids were attached. To seal the crucibles so as to minimize the volatility of sodium, boron, and other critical glass-precursor constituents, tight fitting alumina crucible lids were coated with a glass frit and placed on the crucible in the heat-treatment furnace. In some cases, a nitrogen sweep gas (≈2300 mL/min) was used to purge the region above the top of the melt. Heat treatments were performed by ramp heating from between room temperature and 150°C to 240°C at 3°C/min and then from 300°C to 1150°C at 6°C/min, held at 1150°C for 1 h, and quenched to room temperature. Glass samples were broken from the crucible, ground in a tungsten-carbide mill, fused in $Na_2O_2$ and KOH, dissolved in $HNO_3$, and then analyzed by inductively coupled plasma-optical emission spectrometry (ICP-OES).

The results of these experiments are detailed in a companion report (Peeler et al. 2001), but are summarized here for discussion purposes. Based on comparisons between targeted and measured compositions, it was found that when no nitrogen sweep gas was employed, between 78% (for the SBW-4 additive mix) and 103% (for the SBW-9 additive mix) of the S in the feed was retained in the final glass after vitrification. When a nitrogen sweep gas was used during the vitrification experiments, only an average of 23% was retained in the final glass.

## 2.5 Thermodynamic Model Calculations

### 2.5.1 Approach and Results

We employed the FACT™ computer program to calculate the products that might be generated during the early stages of vitrification of SBW waste at thermodynamic equilibrium. Our goal was to model the reactions occurring under aqueous and hydrothermal conditions and during waste dry out. From the results presented in the sections above, this could best be accomplished by modeling to temperatures of about 270 to 280°C. FACT can perform calculations on aqueous systems up to 270°C; above that, species are partitioned either to gas or solid phases.

Table 2.3 lists the compounds and their amounts used in the first-level calculations for 1 L of simulated SBW waste. FACT is limited in the number of variables that it can handle, so aqueous compounds below a concentration of 0.01 M in the SBW were not included as inputs. Furthermore, there was no reasonable $Fe^{3+}$ aqueous species included in the FACT database, so iron was also excluded from the initial calculations. All solid compounds (e.g., glass precursors, etc.) were excluded as initial FACT inputs as well. These components will be included in subsequent models (see below).

**Table 2.3. Starting Base Feed Composition Used in First-Level Calculations**

| Compound | state | moles |
|---|---|---|
| $H_2O$ | liq | 55.5 |
| $NaNO_3$ | s | 2.12 |
| $Al(NO_3)_3(H_2O)_6$ | s | 0.628 |
| $Ca(NO_3)_2(H_2O)_4$ | s | 0.00453 |
| $Mg(NO_3)_2(H_2O)_6$ | s | 0.00114 |
| $HNO_3$ | liq | 0.0874 |
| $H_2SO_4$ | liq | 0.0510 |
| HF | g | 0.00338 |
| HCl | g | 0.00278 |
| $H_3PO_4$ | s | 0.00129 |
| $H_3BO_3$ | s | 0.00116 |

The experimental "conditions" simulated by the FACT program are summarized in Table 2.4. Three different conditions were employed: oxidizing (OX), reducing (RED), and very reducing (VRED). Oxidizing conditions involved just the base-feed composition listed in Table 2.4. Very reducing conditions were obtained by adding ethylene glycol to the feed in the amount indicated in Table 2.4. Ethylene glycol was used in the FACT calculations because sugar was not in the FACT database. Polyols such as ethylene glycol represent a degradation product of sugar hydrolysis and hydrogenolysis, so its use as a sugar surrogate is not unprecedented. Reducing conditions were simulated by editing the FACT database to exclude the formation of very reduced compounds such as $H_2S$ (whose formation has not been observed).

**Table 2.4. Experimental "Conditions" Employed for First-level Calculations. See text for explanations of OX, RED, and VRED. Units are in moles.**

| | Experiment | | |
|---|---|---|---|
| **Item** | **OX** | **RED** | **VRED** |
| base feed, moles | 58.4 | 58.4 | 58.4 |
| $C_2H_4(OH)_2$, moles | 0.00 | 2.47 | 2.47 |
| final temperature, °C | 220 | 240 | 240 |
| species list edits | - | no $H_2S$ | - |

The results from the dry-out tests indicate that reaction temperatures do not exceed 250°C. Furthermore, the results from the ramp heating and quenching studies indicated that "dry-out" reactions were mostly completed between 180°C and 350°C (probably closer to the former). Thus, a temperature range of 220 to 240°C was selected for the calculations (a single temperature could not be used for all "conditions" because FACT was not able to converge in some cases). The results obtained from these FACT calculations are summarized in Table 2.5 and Table 2.6.

**Table 2.5. First-Level Calculations of Off-Gas Species Generated during Theoretical Heat Treatment to 220 to 240°C. Units are in moles.**

| | Experiment | | |
|---|---|---|---|
| **Compound** | **OX** | **RED** | **VRED** |
| $H_2O$ | 59.4 | 65.4 | 65.5 |
| $CO_2$ | - | 3.58 | 3.58 |
| $O_2$ | 2.70 | - | - |
| $N_2$ | 1.08 | 2.05 | 2.05 |
| $H_2$ | - | 0.535 | 0.519 |
| $CH_4$ | - | 0.388 | 0.342 |
| $H_2S$ | - | - | 0.0510 |
| $NH_3$ | - | 0.00183 | 0.00174 |
| $H_3BO_3$ | 0.000203 | 0.000400 | 0.000400 |
| CO | - | 0.000269 | 0.000260 |
| - indicates an insignificant amount. | | | |

These simulated conditions, however, are still not completely representative of what occurs in reality. One thing, in particular, is that additional pertinent species still need to be included in the simulations. This problem can be fixed by removing non-pertinent species from the simulation so that additional ones can be added. From Table 2.6, one can observe that $CaF_2$, $Mg_3B_2O_6$, and $Ca_{10}(PO_4)_6F_2$ form under all experimental conditions. These compounds serve to tie up the $Mg^{2+}$, $PO_4^{3-}$, and $F^-$ ions. Thus, if we assume that these compounds are relatively stable and will form even if additional components are added, we can remove $Mg(NO_3)_2(H_2O)_6$, HF, and $H_3PO_4$ from the list in Table 2.6 and subtract the appropriate amount of $Ca(NO_3)_2(H_2O)_4$ and $H_3BO_3$. This will then allow us to add $SiO_2$, $Fe_2O_3$, and LiOH to the list of compounds to be included in the FACT calculations. Table 2.7 lists the compounds and their amounts used in the second-level calculations for 1 L of simulated SBW waste plus additives.

**Table 2.6. First-Level Calculations of Solid Compounds Remaining After Theoretical Heat Treatment to 220 to 240°C. Units are in moles.**

| | Experiment | | |
|---|---|---|---|
| **Compound** | **OX** | **RED** | **VRED** |
| $NaNO_3$ | 1.94 | - | - |
| $Na_2CO_3$ | - | 0.972 | 1.02 |
| $NaAl_9O_{14}$ | 0.0698 | 0.0698 | 0.0698 |
| $Na_2SO_4$ | 0.0510 | 0.0510 | - |
| NaCl | 0.00278 | 0.00278 | 0.00278 |
| $CaF_2$ | 0.00148 | 0.00148 | 0.00148 |
| $CaCO_3$ | - | 0.000907 | 0.000907 |
| $Ca(OH)_2$ | 0.000806 | - | - |
| $Mg_3B_2O_6$ | 0.000380 | 0.000380 | 0.000380 |
| $Ca_{10}(PO_4)_6F_2$ | 0.000215 | 0.000215 | 0.000215 |
| $CaB_2O_4$ | 0.0000985 | - | - |
| - indicates an insignificant amount. | | | |

**Table 2.7. Starting Base Feed Composition used in Second-level Calculations. Units are in moles.**

| Compound | State | Waste | Additive | Total |
|---|---|---|---|---|
| $H_2O$ | liq | 55.5 | | 55.5 |
| $SiO_2$ | s | | 2.48 | 2.48 |
| $Fe_2O_3$ | s | 0.0102 | 0.160 | 0.170 |
| $NaNO_3$ | s | 2.12 | | 2.12 |
| $Al(NO_3)_3(H_2O)_6$ | s | 0.628 | | 0.628 |
| LiOH | s | | 0.284 | 0.284 |
| $KNO_3$ | s | 0.185 | | 0.185 |
| $Ca(OH)_2$ | s | 0.000905 | 0.0759 | 0.0768 |
| $H_3BO_3$ | s | 0.000400 | 0.731 | 0.731 |
| $HNO_3$ | liq | 0.0874 | | 0.0874 |
| $H_2SO_4$ | liq | 0.0510 | | 0.0510 |
| HCl | g | 0.00278 | | 0.00278 |

The conditions simulated by the FACT program for these second-level calculations are summarized in Table 2.8. Three different conditions were employed: slightly reducing (SLRD), VRED, and RED. All conditions involved the base-feed composition listed in Table 2.7 plus ethylene glycol (see Table 2.8). Very reducing conditions were simulated by editing the FACT database to exclude the formation of $N_2$ (which was not observed in any of the off gas analyses), $NH_4$, and other highly reduced compounds such as those already discussed (e.g. $H_2S$). Slightly reducing conditions were simulated by editing the FACT database to exclude the formation of $N_2$ and $NH_4$ as well as $CH_4$, $H_2$, $C_2H_4O$, $C_2H_3OOH$, and related compounds. Reducing conditions were simulated by editing the FACT database to exclude the formation of $N_2$, $NH_4$, $CH_4$, and $H_2$, but still allows for the formation of $C_2H_4O$ and $C_2H_3OOH$.

**Table 2.8 Experimental "Conditions" Employed for Second-level Calculations. Units are in moles.**

| | Experiment | | |
|---|---|---|---|
| **Item** | **SLRED** | **RED** | **VRED** |
| base feed, moles | 62.3 | 62.3 | 62.3 |
| $C_2H_4(OH)_2$, moles | 2.47 | 2.47 | 2.47 |
| final temperature, °C | 220 | 220 | 230 |
| Species list edits | no $N_2$, $NH_4$, $CH_4$, $H_2$, $C_2H_4O$, $C_2H_3OOH$ | $C_2H_4O$, $C_2H_3OOH$; no $N_2$, $NH_4$, $CH_4$, $H_2$ | no $N_2$, $NH_4$ |

The results obtained from these FACT calculations are summarized in Table 2.9 through Table 2.12. Focusing just on the RED experimental conditions, Table 2.12 summarized the gas species and their amounts calculated at 240°C, 270°C (the temperature limit for aqueous calculations), and 280°C (where all species are partitioned either to the gas or solid phases).

**Table 2.9. Second-Level Calculations of Off Gas Species Generated During Theoretical Heat Treatment to 220 to 230°C. Units are in moles.**

| | Experiment | | |
|---|---|---|---|
| **Compound** | **SLRED** | **RED** | **VRED** |
| $H_2O$ | 68.3 | 66.8 | 66.4 |
| CO | 3.22 | 0.113 | 0.00015 |
| $N_2O$ | 2.22 | 2.22 | 2.22 |
| $CO_2$ | 1.18 | 2.76 | 3.69 |
| $CH_4$ | - | - | 0.749 |
| $H_2$ | - | - | 0.535 |
| $C_2H_3OOH$ | - | 0.540 | - |
| $C_2H_4O$ | - | 0.187 | - |
| $H_3BO_3$ | 0.00626 | 0.00785 | 0.00808 |
| $[HBO_2]_3$ | (a) | (a) | (a) |
| HCOOH | - | (a) | - |
| $SO_2$ | - | (a) | - |
| (a) amount is between $10^{-6}$ and $10^{-8}$ moles.<br>- indicates an insignificant amount. | | | |

**Table 2.10. Second-level Calculations of Major Aqueous Species Remaining After Theoretical Heat-treatment to 220-240°C. Units are in moles.**

| | Experiment | | |
|---|---|---|---|
| **Compound** | **SLRED** | **RED** | **VRED** |
| $H_2O$ | 0.0247 | 0.0249 | - |
| $Na^+$ | 0.0459 | 0.0473 | - |
| $S_2O_3^{2-}$ | 0.0255 | 0.0255 | - |
| $K^+$ | 0.00461 | 0.00525 | - |
| $Li^+$ | 0.000546 | 0.000732 | - |
| $Cl^-$ | 0.0000573 | 0.0000499 | - |
| $CH_3COO^-$ | - | 0.00226 | - |
| - indicates an insignificant amount. | | | |

**Table 2.11. Second-level Calculations of Solid Compounds Remaining After Theoretical Heat-treatment to 220-240°C. Units are in moles.**

| | Experiment | | |
|---|---|---|---|
| **Compound** | **SLRED** | **RED** | **VRED** |
| $Na_2CO_3$ | 0.540 | 0.605 | 0.501 |
| $NaAlSi_3O_8$ | 0.448 | 0.448 | 0.443 |
| $Na_2B_4O_7$ | 0.181 | 0.181 | 0.181 |
| $KAlSi_3O_8$ | 0.180 | 0.180 | 0.185 |
| $Fe_2SiO_4$ | 0.170 | 0.170 | - |
| $Fe_3O_4$ | - | - | 0.113 |
| $Li_2Si_2O_5$ | 0.142 | 0.131 | 0.142 |
| $Na_2Si_2O_5$ | 0.0653 | - | 0.0790 |
| $Na_2SO_4$ | - | - | 0.0510 |
| $Na_2Ca_3Si_6O_{16}$ | 0.0256 | 0.0256 | 0.0256 |
| $Li_2SiO_3$ | - | 0.0109 | - |
| NaCl | 0.00278 | 0.00273 | 0.00278 |
| - indicates an insignificant amount. | | | |

**Table 2.12. Second-level Calculations of Off Gas Species Generated During Theoretical Heat-treatment to 240-280°C. Units are in moles.**

| | Temperature | | |
|---|---|---|---|
| **Compound** | **240°C** | **270°C** | **280°C** |
| $H_2O$ | 66.9 | 67.0 | 67.1 |
| $CO_2$ | 2.82 | 2.75 | 2.70 |
| $N_2O$ | 2.22 | 2.22 | 2.22 |
| CO | 0.159 | 0.380 | 0.496 |
| $C_2H_4O$ | 0.217 | 0.296 | 0.325 |
| $C_2H_3OOH$ | 0.492 | 0.338 | 0.299 |
| $H_3BO_3$ | 0.00809 | 0.00860 | 0.00875 |
| $SO_2$ | * | $1.23 \times 10^{-6}$ | $11.0 \times 10^{-6}$ |
| HCOOH | * | * | $1.08 \times 10^{-6}$ |
| $[HBO_2]_3$ | * | * | * |
| HCl | * | * | * |
| * amount is between $10^{-6}$ and $10^{-8}$ moles. | | | |

Note from Table 2.12 that $SO_2$(g) is generated in amounts greater than $1 \times 10^{-6}$ moles at and above 270°C. At higher temperatures, the complexity of the calculations due to the large number of species often does not allow FACT to converge on an answer. Thus, we took the approach of starting with an intermediate feed—one based on the solid compounds that remain after theoretical heat treatment of the base feed to 280°C under reducing conditions. This also acts to mathematically purge the gases formed from the decomposition of the base feed—something that one might expect to happen physically anyway

since sweep gases have been used in much of the experimental work presented so far. This intermediate feed composition is listed in Table 2.13.

**Table 2.13. Intermediate Feed Composition Used in Additional Second-Level Calculations**

| Compound | State | Moles |
|---|---|---|
| $NaAlSi_3O_8$ | s | 0.443 |
| $Na_2CO_3$ | s | 0.430 |
| $KAlSi_3O_8$ | s | 0.185 |
| $Na_2B_4O_7$ | s | 0.180 |
| $Na_2SiO_5$ | s | 0.150 |
| $Li_2SiO_3$ | s | 0.142 |
| $Fe_3O_4$ | s | 0.113 |
| $Na_2SO_4$ | s | 0.0510 |
| $Na_2Ca_3Si_6O_{16}$ | s | 0.0256 |
| NaCl | s | 0.00278 |

Table 2.14 lists the gas species and their amounts generated after theoretically heat treating the intermediate feed listed in Table 2.13 to 1150°C. Also note the results obtained if one replaces the $Na_2SO_4$ in the intermediate feed with $Na_2SO_3$ (i.e., a reduced form of sulfur). Reduced sulfur species have been calculated to exist in the aqueous phase of heat-treated base feed (see Table 2.10). Experimentally, extreme hydrothermal treatment of zirconium sulfate solutions have yielded sulfated zirconia powders containing both $SO_4^{2-}$ and $SO_3^{2-}$ (Matson et al. 1998). So the possibility of reduced species surviving beyond 270°C (where FACT has to turn off the aqueous phase calculations, and the reduced sulfur species may artificially be re-oxidized to sulfate) may be significant. The results from Table 2.14 indicate that between 32.4% (for the $Na_2SO_4$ containing feed) and 99.9% (for the $Na_2SO_3$ containing feed) can potentially become volatilized after heat treatment to 1150°C. Of course, these calculations do not take into account either the miscibility of $Na_2SO_4/Na_2SO_3$(l) and molten glass or the solubility of $Na_2SO_4/Na_2SO_3$ in the molten glass.

**Table 2.14. Additional Second-Level Calculations of Off Gas Species Generated During Theoretical Heat-Treatment to 1150°C. Units are in moles.**

| | Sulfur Source | |
|---|---|---|
| **Compound** | **$Na_2SO_4$** | **$Na_2SO_3$** |
| $SO_2$ | 0.0165 | 0.05097 |
| $SO_3$ | $20.2\times10^{-6}$ | $21.7\times10^{-6}$ |
| $Na_2SO_4$ | $4.7\times10^{-6}$ | $5.1\times10^{-6}$ |
| SO | $0.073\times10^{-6}$ | $0.642\times10^{-6}$ |
| $K_2SO_4$ | $0.066\times10^{-6}$ | $0.071\times10^{-6}$ |
| $Li_2SO_4$ | $0.043\times10^{-6}$ | $0.046\times10^{-6}$ |

# 3.0 Melter Tests

Three melter tests were performed with simulated SBW feeds in two melter systems—the RSM and the Envitco EV-16. These tests are described in Sections 3.1 through 3.3 along with a highlight of their results. Section 3.4 compares the laboratory-scale tests with those of the melter tests.

## 3.1 EV-16-1999-1 Test

The EV-16 melter at Clemson University has a 45.7 × 45.7 cm melt chamber, with a design depth of 40.6 cm and a flat bottom. The melter was lined with Unicor 501, fused cast alumina-zirconia-silica (AZS) refractory. A sloped bottom was installed using a ram-formed Narco Zirmul 160 patch. In this configuration, the working volume of the melter is approximately 55 L. The refractory melt chamber is encased in a shell of segmented water-cooled panels. The superstructure of the melter is enclosed in a stainless steel hood, lined with 75 mm of high-temperature fiberboard insulation. The hood is fitted with access doors that permit the operator to observe the cold-cap and/or melt-surface characteristics, take glass or cold-cap samples, or add additional materials to the melt surface. The molten glass is drained from the bottom of the melter using a heated orifice. Flow rates are controlled by adjusting the orifice temperature through heating and/or cooling as necessary. The orifice currently contains a plunger. Electrical power is applied to the melter through a 100-kVA power supply, which uses a Scott-T transformer to convert the three-phase power to a balanced two-phase input to the furnace. Power is applied to the bath through four 32-mm molybdenum electrodes that enter the melter horizontally through each of the four sides of the melt chamber. The electrodes are installed through water-cooled holders, thereby allowing the operator to adjust or advance the electrodes in case of wear or process changes. A variable-speed tubing pump delivered the feed to the melter through a 6.35-mm (0.25-in.) stainless steel feed tube. A mechanical agitator in the feed tank was used to ensure homogenous suspension of solids in the slurry feed. The feed tube, which entered the melter from a penetration in the rear face of the hood, is manually positioned to deposit the feed in the desired location in the melter. A diagram of the melter (with the sloped bottom installed) is provided in Figure 3.1. The off-gas treatment system for the EV-16 is a multi-stage wet scrubber, designed to handle particulate matter and acid gases. The off-gas system is constructed of 304 stainless steel and PVC and consists of a quench chamber, steam/air atomizing scrubber, cyclonic separator, scrubbing column, demister, and rotary blower.

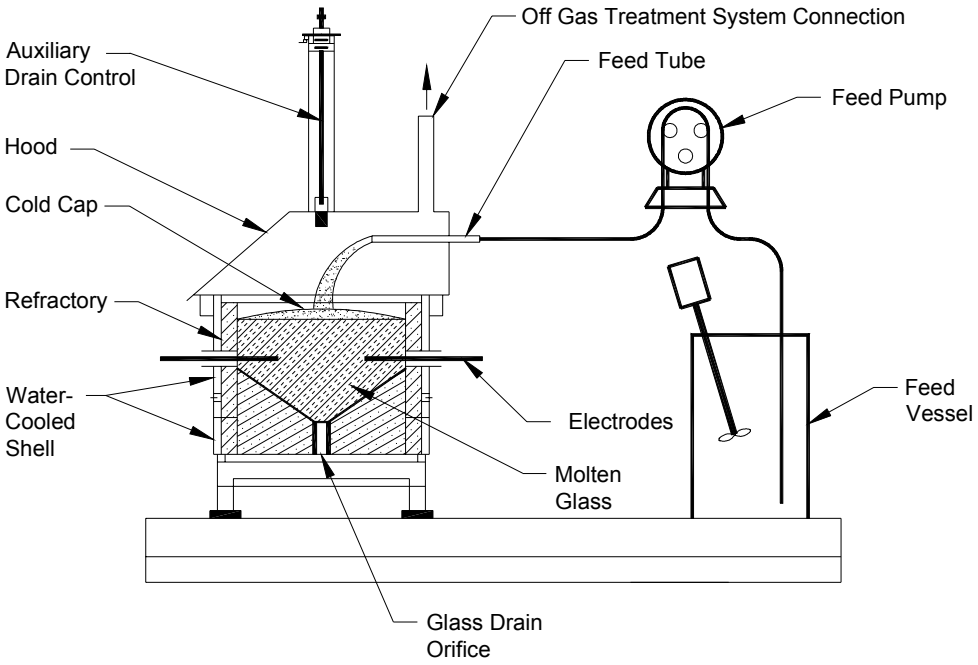


**Figure 3.1. Schematic of the EV-16 Melter (after Musick et al. 2000)**

The EV-16-1999-1 test was performed in April 1999 using the 1998 SBW simulant composition with glass-forming additives of SBW-1 and a target waste loading of 35 mass% based on the recommendation of Vienna et al. 1999. Carbon in the form of powdered activated carbon was added to the feed at 87.4 g/L to ensure adequate reduction of transition elements to avoid undue corrosion of the melter electrodes and ensure nitrate destruction for less problematic melting. The test was performed over a period of just less than 3 days with a time-average feeding rate of 135 mL/min. Over the duration of the test, 450 L of feed were fed to the melter, producing 155 kg of glass. The target melt-pool temperature was 1150°C. However, temperature excursions of up to 1350°C occurred throughout the test due to a faulty temperature control device.

Analyses of the resulting glass by X-ray fluorescence spectroscopy (XRF) and by ICP showed a $SO_3$ concentration of 0.49 mass% and 0.58 mass%, respectively. The target concentration of $SO_3$ in glass was 1.3 mass%, and ICP analyses of the melter feed suggests an *as-batched* $SO_3$ concentration of 1.07 mass%. This suggests that 54% of the S fed to the melter was in the glass (based on ICP measured results of the feed and the glass). No evidence of a salt layer was seen at the melt surface during or after the test.[(e)] Insufficient data were collected to determine the amount and speciation of S in the off gas. However, it is likely that the remaining fraction of the S fed to the melter partitioned to the off gas.

## 3.2 RSM-01-1 Test

The RSM is a 15.24-cm (6-in.) diameter, joule-heated melter capable of continuous feeding and pouring that was specifically designed and built to evaluate various aspects of the vitrification process. The RSM consisted of a 26-cm (10.25 in.) outside diameter × 44.45-cm (17.5 in.) high Inconel 601 shell,

[(e)] The absence of a salt phase during this test may have been influenced by the temperature excursions.

lined with ceramic paper and Alfrax 66. A crucible of Monofrax K-3 high $Cr_2O_3$ refractory provided a melt cavity that measures 15.24 cm (6 in.) in diameter. The operating glass height of the RSM is nominally 7.6 cm (3 in.) resulting in a glass volume of 1.4 L. Additional external heating is provided by a kiln to overcome heat losses to the surroundings. Power to the RSM is provided by two, top-entering paddle electrodes. The electrode paddles are made from 0.64 cm (0.25 in.) Inconel 690 plate. The face of the electrode paddles measured 7.6 cm x 7.6 cm (3-in. x 3-in.) and extended to the bottom of the melter through the melter lid. Half of an Inconel tube is welded to the backside of each electrode, providing a thermowell for a type K thermocouple in an Inconel sheath. The thermowell is attached to the backside of the electrode to prevent upsets in the processing behavior of a melter. Alfrax 66 is used to stabilize the electrodes in the melter lid and electrically isolate the electrodes from the melter shell. Feed is pumped from a feed tank using a peristaltic pump and is introduced into the melter via a cooled nozzle. A view port in the lid allowed observations of the cold cap, observations of salt-layer formation, and sampling from the melt surface. The off gas-system included a film cooler, venturi scrubber, high-efficiency mist eliminator, and scrub-solution tank. Characterization of process off-gas effluent emission rates and equipment abatement efficiencies are accomplished using gaseous and particulate samplers operated according to applicable U.S. Environmental Protection Agency (EPA) protocols. In addition, an online quadrupole MS allowed real time analysis to be conducted for volatile and semivolatile effluents having mass numbers between 2 and 300 AMU. The discharge section of the RSM relies upon an Inconel overflow pipe and gravity for glass removal from the RSM. The overflow tube is heated to facilitate glass pouring. Canisters that collect the glass from the overflow are heated to promote slumping of the glass in the canister. Figure 3.2 shows a schematic of the RSM.

The RSM-01-1 test was performed in January 2001 using the 2000 WM-180 simulant composition with glass-forming additives of SBW-9. The target waste loadings were increased from 30 to 35 mass% during the eight test segments to determine the loading at which a salt layer would accumulate (see Table 3.1). The amount of S was increased by 40% during the final segment to intentionally form a salt layer. Sugar was added as a reductant at concentrations ranging from 135 to 197 g/L of SBW to get an initial assessment of the impacts of reductant concentration on S loss and glass redox. The test was performed over a period of 120 h with a feeding rate of 2.1 to 3.3 L/h and a glass pour rate of 35 to 54 $Kg/h/m^2$. The average oxide loading of the feed was 292 g/L. The melt-pool temperature was maintained between 1147 and 1162°C with a target nominal melt temperature of 1150°C.

Goles et al. (2001) thoroughly described the results of the RSM-01-1 test. Table 3.2 compares the ICP analyses of $SO_3$ in glass with target values. Roughly, 50 to 60% of the S fed to the melter partitioned to the glass and is apparently relatively independent of waste loading in the range of 30 to 35 mass%. A mass balance over the entire 120-h test found that roughly 25% of the S fed to the melter partitioned to the off-gas system, roughly 80% of which was found in the drainage from the high-efficiency mist eliminator (HEME), and the remaining was in the scrub solution. More of the S could have been in the HEME since the entire HEME was not flushed after the test. Alternatively, if the remaining 15 to 25% of the S left the melter as $SO_2$, the concentration of $SO_2$ would have been below the detection limit of the MS used to monitor off-gas composition. Small areas of molten salt were seen on the melt surface during the entire test. However, salt accumulation was not seen until the waste loading was increased to 35%. Although no accurate data were taken to quantify the amount of salt accumulation, visual observations suggested that the amount of salt on the melt surface decreased when the amount of sugar increased during the last test segment.

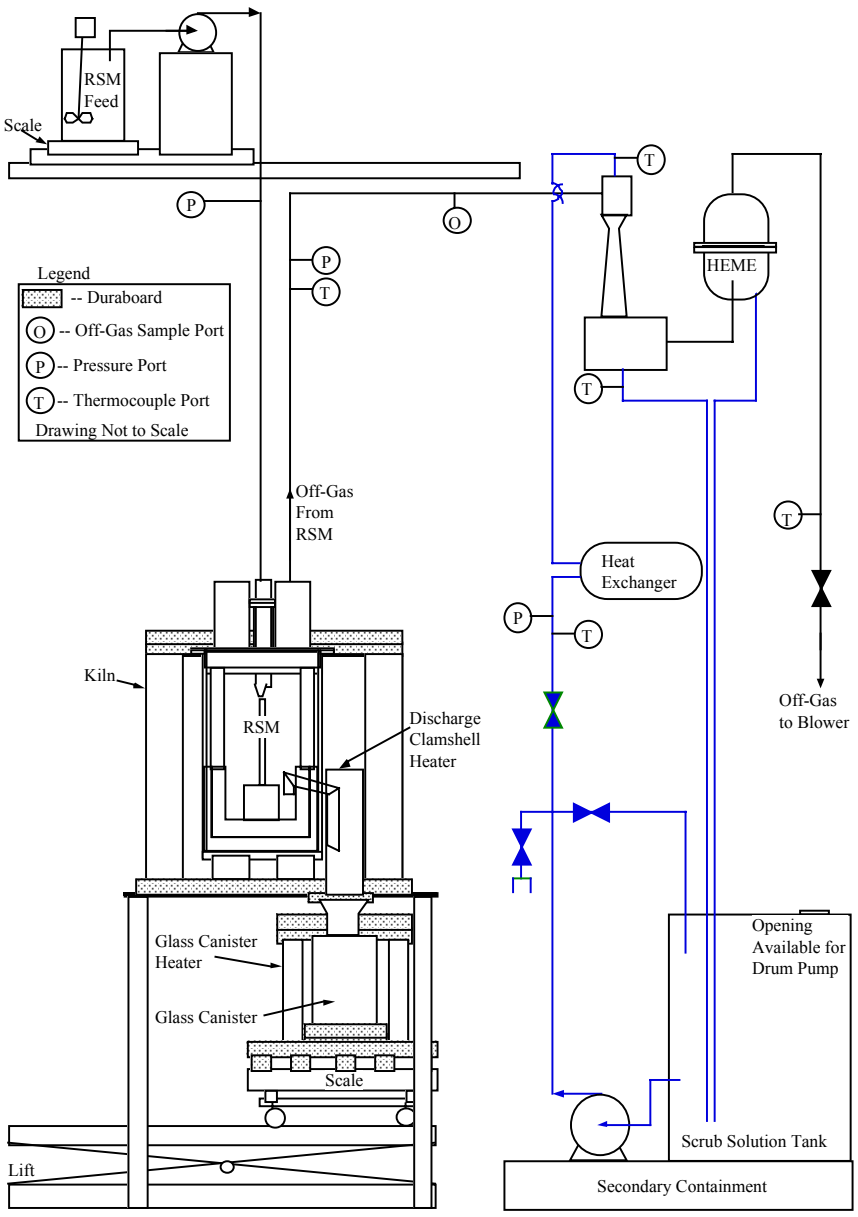


**Figure 3.2. Schematic of the Research-Scale Melter System (after Goles et al. 2001)**

**Table 3.1. Summary of RSM-01-1 Segments**

| Segment | Waste Loading (mass%) | Target $SO_3$ Concentration | Sugar Concentration (g/L of SBW) | Feed Rate (L/h) |
|---|---|---|---|---|
| A | 30 | 1.07 | 135 | 2.1 |
| B | 30 | 1.07 | 135 | 2.3 |
| C | 32 | 1.14 | 135 | 3.0 |
| D | 32 | 1.14 | 135 | 2.8 |
| E | 35 | 1.25 | 135 | 2.5 |
| F | 35 | 1.25 | 150 | 2.6 |
| G | 35 | 1.25 | 155 | 3.2 |
| H | 35 | 1.75 | 178 | 3.3 |

**Table 3.2. Summary of S Content in RSM-01-1 Glass**

| Waste Loading (mass%) | Target $SO_3$ in Glass (mass%) | Measured $SO_3$ in Glass (mass%) | % of S in Glass |
|---|---|---|---|
| 30 | 1.07 | 0.68 | 63 |
| 32 | 1.14 | 0.66 | 56 |
| 35 | 1.25 | 0.70 | 56 |
| 35 (1.40×S) | 1.75 | 0.89 | 51 |

## 3.3 EV-16-2001-1 Test

A second melter test was performed in the EV-16 pilot-scale melter (described in Section 3.1) in April of 2001. Prior to the test, the melter plenum was rebuilt, and other melter modifications were made, which will be described in the near future.[(d)] This test, EV-16-2001-1, processed a glass using the 2000 WM-180 waste simulant at 30 mass% loading with the SBW-9 additive mix. Sugar was added as a reductant to the feed at concentration of 160 g/L of SBW. With the exception of the sugar concentration, this feed composition is the same as that processed in the RSM-01-1 test during the first two segments. This test was performed over 175 h with active feeding for approximately 120 h. The average nominal feeding rate was 14.7 L/h. Approximately 1790 L of feed was fed during the test, and 538 kg of glass were produced. The empirical oxide loading of the feed was 21.9%. The melt pool temperature was maintained between 1100°C and 1175°C with a nominal target of 1150°C.

The analyses of test samples are ongoing and will be published along with the detailed test description and results in the near future.[(f)] The concentration of S in glass mined from the melter was measured by XRF and ICP. Table 3.3 compares the measured concentrations of $SO_3$ with the target values. Based on XRF and target concentrations, 72% of the S fed to the melter was found in the glass.

[(f)] K. J. Perry, et al. *Test results from SBW-FY01-PS-1, Vitrification Demonstration of Sodium Bearing Waste Simulant Using WM-180 Surrogate*, to be Published August 30, 2001. Idaho National Engineering and Environmental Laboratory, Idaho Falls, Idaho.

The difference between the 63% and 72% S retention in the final glass between the RSM-01-1 and EV-16-2001-1 tests targeting the same waste loading may be due to the differences in melter feed rate, melter design (e.g., melt depth, melter shape), gas-flow rate over the melt, analytical error, and/or other parameters. Normalizing the feed rate to the melter surface area, the average RSM-01-1 feed rate was 120 L/h/$m^2$ and that for the EV-16-2001-1 was 70 L/h/$m^2$.[(g)] With slower feeding, there is more opportunity for the melt to approach the equilibrium concentration of $SO_3$, which is estimated to be roughly 1 mass% for this melt composition in air.

A molten salt was found to form and possibly accumulate during the EV-16-2001-1 test, unlike the EV-16-1999-1 and RSM-01-1 tests. A method to measure the amount of salt at the melt pool surface during the test was not available, but qualitative observations were made by probing the melt surface with an alumina tube. However, the amount of salt that remained on the glass surface when the melter was cooled after the test was estimated. This salt layer, which was found on the melter refractory-glass interface, was estimated to contain 7.7% of the S fed to the melter.[(h)] Details of this calculation will be reported later. There is no clear explanation why a salt layer appeared to accumulate in EV-16-2001-1, but not in the previous two tests. The amount and speciation of S in the off gas was not yet available at the time of this report. It is presumed that the remaining S was lost to the off-gas system.

**Table 3.3. Summary of S Content in EV-16-2001-1 Glass**

| Sample | Target $SO_3$ (Mass%) | XRF $SO_3$ (mass%) | ICP $SO_3$ (mass%) |
|---|---|---|---|
| Melter Bottom | 1.07 | 0.74 | 0.79 |
| General Melter Glass | 1.07 | 0.75 | 0.77 |
| Melter Top | 1.07 | 0.76 | 0.76 |

## 3.4 Comparison with Crucible Tests

It is tempting to state that certain laboratory-scale batch crucible experiments involving dried feed coincidentally compare reasonably close (within 10%) to the results obtained from experiments performed in larger, liquid-fed continuous melters. For example, dried SBW feed melted in the quartz crucible setup (SBW-4 feed, 35 mass% waste loading, 141 g sugar per liter of waste simulant, 1.14 mass% $SO_3$ target loading in glass) with a 100-ccm inert sweep gas resulted in a glass S retention value fairly close to that obtained from the RSM-01-1 run (SBW-9 feed, 30 to 35 mass% waste loading, 135 to 155 g sugar per liter of waste simulant, 1.07 to 1.25 mass % S target loading in glass), 64% vs. an average of 58%, respectively. Likewise, dried SBW feed melted in the sealed crucible setup (SBW-4 feed, 35 mass% waste loading, 141 g sugar per liter of waste simulant, 1.14 mass% $SO_3$ target loading in glass) resulted in a glass S retention value fairly close to that obtained from the EV-16-2001-1 run (SBW-9 feed, 30 mass% waste loading, 160 g sugar per liter of waste simulant, 1.07 mass % S target

[(g)] The complexity of melter feed to glass conversion processes does not allow the scaling of melter feed rates between different melters; the feed rate per unit melt pool surface area is often used as a very rough estimate for comparison purposes.

[(h)] The amount of salt on the melter surface after the test was roughly 575 g, and a total of 2594 g of S was fed to the melter. Assuming the salt was composed of 34.77 mass% S, 7.7% of the S fed to the melter would be in the salt.

loading in glass), 78% vs. 72%, respectively. The sulfur content in these samples was determined using the same technique, so based on only that, comparisons would certainly be valid. However, these sets of experiments use different additive mixes (SBW-4 vs. SBW-9) and different sugar contents (141 g/L vs. 160 g/L), thus making a direct comparison difficult. We shall address this further in Section 5, where it will be estimated that when these differences are accounted for, there is actually a significant difference in the glass S retention values.

If the melter operation parameters were already delineated and the only issue was, for example, glass formulation, then in any potential coincidental cases, laboratory-scale crucible experiments performed on dried SBW feed might be a good alternative to costly large-scale testing for initial screening efforts. However, for SBW waste vitrification, other parameters, such as feed rate, are still variables and need to be investigated as well. With the exception of the crucible tests made using an inert sweep gas, these laboratory-scale crucible tests do not allow for significant process variation (e.g., feed rate, plenum temperature). A laboratory-scale melter that emulates the larger, liquid-fed, continuous melters would be a valuable research tool for studying how process variables influence, in the case of SBW vitrification, S partitioning. In the next section, we describe just such a research tool, which we call the centimeter-scale melter (CSM), and the results we obtained from the vitrification of simulated aqueous SBW feed.

# 4.0 Integrated Feed-to-Glass Studies

## 4.1 Test Description

Figure 4.1 shows a schematic diagram of the CSM developed for SBW feed testing.

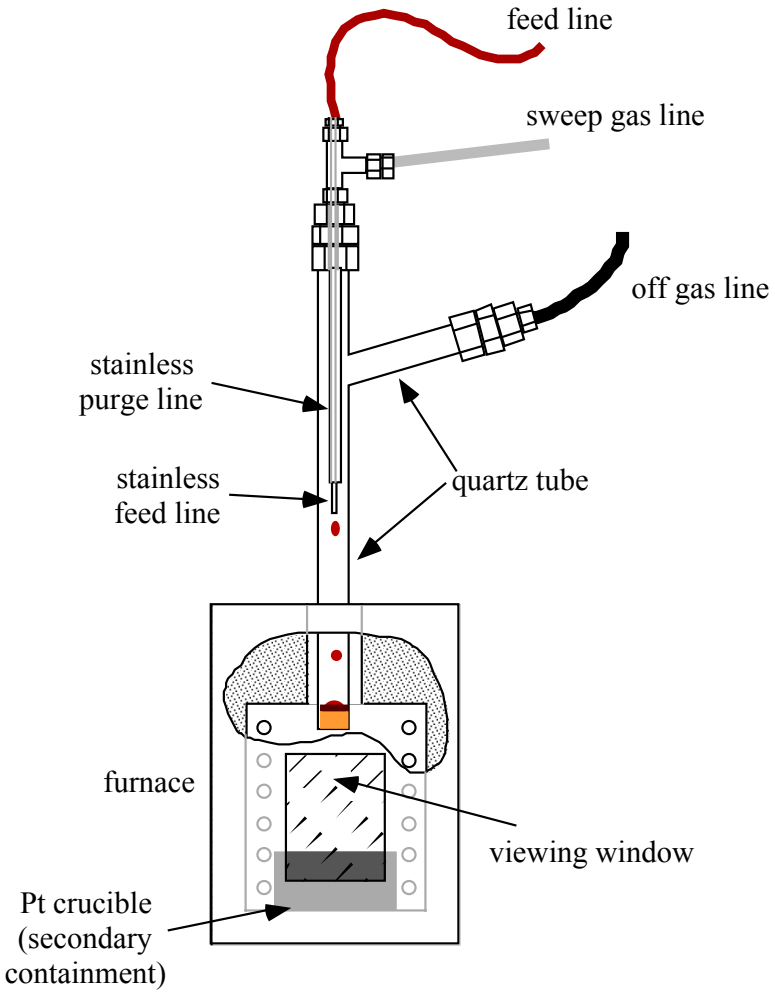


**Figure 4.1. Schematic Diagram of the CSM. The quartz tube assembly is gradually lowered further into the furnace as the melt level increases with time. For clarity, a cut-away view of part of the furnace is shown.**

The CSM is a modification to the quartz crucible setup discussed in Section 2.4.3. Feed is pumped at the desired rate into a quartz crucible through a stainless steel tube. Another stainless steel tube around the feed tube allows sweep gas to flow into the system. The quartz arm extending from the main tube allows for off gas to escape. The whole system is sealed using Swage-Lock fittings.

To make a CSM run, a new quartz-tube assembly is inserted in at the very top of a box furnace as indicated in Figure 4.1. The furnace is brought to equilibrium at the desired temperature (1150°C for all the work discussed in this report), the sweep gas is set to the desired flow rate (see below), and then the feed is pumped into the CSM. As the melt level increases with time, the entire quartz tube assembly is gradually lowered further into the furnace, which maintains heating from the bottom and a lower temperature plenum. When the run is finished, the quartz-tube assembly is completely removed from the furnace and allowed to air cool. Glass samples were broken from the crucible and then analyzed by either XRF or ICP.

A large sample of the RSM-01-1 feed for segments C and D formed the base feed used in initial CSM testing. This feed contains the 2000 WM-180 SBW simulant at 32 mass% loading (on a nonvolatile oxide basis) with SBW-9 additive mix and 135 g of sugar per liter of waste simulant. This feed was used unless otherwise noted. Several different configurations were used to collect the off gas from the CSM. The earliest run (run CSM41201) used the following setup (Configuration A). The off-gas hose was attached to a scrubber bottle, which allowed the gas to bubble through deionized water to (hopefully) remove $H_2SO_4$, $HNO_3$, $SO_3$, etc. The gas output from the scrubber was then passed through a condenser to remove as much water as possible before it was analyzed using a Hewlett Packard model 5890 GC and a model 5971 MS. The GC's Pora PLOT Q column was maintained at 90°C. The gases that were monitored quantitatively included $O_2$, $CO_2$, CO, $SO_2$, NO, $N_2O$, and $CH_4$. The GC-MS data were very noisy, presumably due to the pressure fluctuations in the off gas and perhaps the large quantity of water in the off gas. In any event, no $SO_2$ was detected in the off gas from run CSM41201.

In the next configuration (Configuration B), the GC-MS gas analysis was not performed. The off gas was first passed through a stainless steel radiating coil to cool the hot gases and then simply bubbled through the scrubber bottle and vented to the fume hood. In the final configuration (Configuration C), GC/MS gas analyses was again used, but using a modified setup: the off-gas hose was attached first to a condenser. The gas output from the condenser was then split into two parts: one part (≈10% of the gas flow) went directly to the GC-MS, and another part was passed through the scrubber bottle. The gas output from the scrubber was then vented to the fume hood.

A summary of all the relevant CSM runs along with additional experimental details is given in Table 4.1.

**Table 4.1. Summary of Relevant CSM Runs**

| Run | Description | Summary | Chemicals Added per 100 mL of base feed | Configuration | Feed Rate (mL/min) | He/2%Ar Flow Rate (ccm) |
|---|---|---|---|---|---|---|
| CSM41201 | base run | | | | 0.8 | 50 |
| CSM42701 | base run | | | B | 1.5 | 100 |
| CSM62101 | $SO_2$ spikes | $SO_2$ injected during run | | C | 1.3 | 300 |
| CSM62701 | $SO_2$ spikes | $SO_2$ injected during run | | C | 1.3 | 300 |
| CSM62201 | long run | 200mL total feed | | C | 1.3 | 300 |
| CSM50801 | fast purge | | | B | 1.5 | 1000 |
| CSM60101 | slow feed | | | C | 0.5 | 100 |
| CSM51401 | fast feed | | | B | 7.2 | 100 |
| CSM53101 | no sugar | 0% C (sugar) | (no sugar used) | C | 1.3 | 100 |
| CSM60601 | low sugar | 50% C (sugar) | 6.75g sugar | C | 1.3 | 100 |
| CSM60801 | high sugar | 150% C (sugar) | 20.24g sugar | C | 1.3 | 100 |
| CSM62601 | high C+$NO_3^-$ | 150% C, fixed C/$NO_3^-$ | (150% C, fixed C/$NO_3^-$) | C | 1.3 | 300 |
| CSM61801 | sugar + urea | 100% C | (sugar + urea) | C | 1.3 | 300 |
| CSM61201 | glycolic | 83%C (glycolic acid) | 14.88g glycolic acid | C | 1.3 | 100 |
| CSM51601 | high $SO_4^{2-}$ | 200% $SO_4^{2-}$ ($Na_2SO_4$) | 0.69g $Na_2SO_4$(s) | B | 1.3 | 100 |
| CSM61401 | high acid | 240% $H^+$ ($HNO_3$) | 9.1mL 15.4M $HNO_3$ | C | 1.3 | 300 |
| CSM52401 | high acid | 240% $H^+$ ($HNO_3$) | 10mL 15.4M $HNO_3$ | B | 1.5 | 100 |

## 4.2 Results and Discussion

A quantitative analysis of the salt layers formed (if applicable) during the CSM runs was not attempted. This is because the quartz crucible and glass within it fracture considerably when cooled, producing many small fragments. Qualitatively, however, we can still make some general, yet subjective, observations about the relative degree of salt coverage on the melt surface. These observations are summarized in Table 4.2. The only process variable that had a large effect on the degree of surface coverage was the feed rate—a high feed rate (CSM51401) generated considerable salt coverage whereas a moderate (CSM42701) or slow (CSM60101) feed rate produced significantly less salt coverage.

In terms of the effect of feed chemistry on the degree of salt coverage, greater sulfate concentrations (CSM51601) produced a glass with slightly greater salt coverage compared to baseline runs. Greater sugar (CSM60801), nitric acid (CSM61401and CSM52401), or both (CSM62601) produced glasses with insignificant salt coverage.

The sulfur content in the glasses produced from the CSM was analyzed by either XRF or ICP. The results obtained to date are listed in Table 4.3. For two samples (CSM42701 and CSM51401), S retention values were determined using both methods. We found a consistent difference in results between the two methods, with the ICP analysis giving roughly 51% to 69% larger values compared to the XRF data. In contrast, for the analysis of the EV-16-1999-1 glass using both techniques (see above), the ICP S retention value is only about 17% larger that the XRF value. These differences need to be addressed in ongoing work. For now, to alleviate these technique-related differences in S retention numbers, we report the effects of process and chemistry variation on the S retention as the percentage deviation, $\Delta$ (%), from a baseline average (48.5% for XRF and 73.2 for ICP). These calculations are also reported in Table 4.3.

As can be seen from Table 4.3, the largest effect on S retention is due to variations in the sugar concentration in the feed—a high sugar content (CSM60801) yielded a glass with much less S retained, and lower (CSM60601) or no sugar (CSM53101) content yielded glasses with significantly ($\Delta > 10\%$) greater S retention, as indicated in Figure 4.2. Also shown in Figure 4.2 is the influence of sugar concentration on the iron redox of the resulting glass. Although over 70% of the target S can be partitioned to the off gas using high sugar concentrations, the resulting glass would have a redox ratio of roughly 80% Fe(II)/total Fe. Interestingly, feeds containing no or low sugar exhibited batch expansion during vitrification; no other runs behaved in this manner.

**Table 4.2. Qualitative Observations of Salt Coverage for CSM Runs**

| | | Degree of Salt Coverage | | | | |
|---|---|---|---|---|---|---|
| **Run** | **Description** | **0** | **1** | **2** | **3** | **4** |
| CSM41201 | base run | | | | | |
| CSM42701 | base run | | | | | |
| CSM62101 | base run | | | | | |
| CSM62201 | long run | | * | | | |
| CSM50801 | fast purge | | | | | |
| CSM60101 | slow feed | | * | | | |
| CSM51401 | fast feed | | | | | |
| CSM53101 | no sugar | | | | | |
| CSM60601 | low sugar | | * | | | |
| CSM60801 | high sugar | | | | | |
| CSM62601 | high $C+NO_3^-$ | | | | | |
| CSM61801 | sugar + urea | | * | | | |
| CSM51601 | high $SO_4^{2-}$ | | | | | |
| CSM61401 | high acid | | | | | |
| CSM52401 | high acid | | | | | |

Degree of salt coverage: (0) insignificant, (1) salt at the melt/crucible interface only, (2) salt coverage begins to intrude slightly on the interior surface region, (3) still more interior surface region coverage by salt, and (4) relatively severe salt coverage.

* indicates that an unusual looking surface was observed—not a salt layer, but what appears to be unreacted feed that might have dribbled onto the melt surface after the run was finished.

A dashed vertical line represents an approximate average degree of salt coverage for base runs.

**Table 4.3. Analytically Determined Values of S Retention in Glass for CSM Runs**

| | | Target $SO_3$ in Glass | Measured mass% $SO_3$ in Glass | | S retention (% of Target S in glass) | | Δ |
|---|---|---|---|---|---|---|---|
| **Run** | **Description** | **(mass%)** | **XRF** | **ICP** | **XRF** | **ICP** | **( %)[a]** |
| CSM41201 | Base run | 1.14 | 0.55 | | 48.0 | | -1 |
| CSM42701 | Base run | 1.14 | 0.55 | 0.84 | 48.5±2.9[b] | 73.2 | 0 |
| CSM50801 | Fast purge | 1.14 | 0.51 | | 44.7 | | -8 |
| CSM60101 | Slow feed | 1.14 | | 1.06 | | 93.0 | +27 |
| CSM51401 | Fast feed | 1.14 | 0.48 | 0.81 | 41.9 | 71.1 | -3[c] |
| CSM53101 | No sugar | 1.14 | | 1.14 | | 100.0 | +37 |
| CSM60601 | Low sugar | 1.14 | | 1.10 | | 96.1 | +31 |
| CSM60801 | High sugar | 1.14 | | 0.35 | | 30.7 | -58 |
| CSM51601 | High $SO_4^{2-}$ | 2.28 | 0.68 | | 29.7 | | -39 |
| CSM61401 | High acid | 1.14 | | 0.88 | | 77.4 | +6 |
| CSM52401 | High acid | 1.14 | | 0.81 | | 70.6 | -4 |

(a) Δ, in %, is equal to 100×(S retention of the glass sample—48.5)/48.4 for the glasses analyzed by XRF or 100×(S retention of the glass sample—73.2)/73.2 for the glasses analyzed by ICP.

(b) this entry is the average of three separate measurements on different regions of the prepared glass (top without salt, middle, and bottom).

(c) Δ, in %, is -14 for the XRF analyzed sample and -3 for ICP.

The feed rate also influenced the S retention in the final glass; a slow feed rate (CSM60101) increased Δ significantly.

The sweep-gas flow rate, however, had little effect on the S retention in the final glass for CSM runs. In comparing, for example, the run made with 100-ccm sweep gas (CSM42701) and that made with 1000-ccm sweep gas (CSM50801), we also need to factor in the amount of batch gas that is being generated. As will be discussed in Section 4.3, we can expect a batch-gas evolution rate of about 1200 ccm. This means that in comparing runs CSM42701 and CSM50801, we are looking at the difference between about 1300 ccm and 2200 ccm total gas flow rate respectively. Thus, the effect of gas flow rate on the partitioning of S to the final glass for CSM runs (and perhaps more generally to all liquid fed melter runs) is minimal; increasing the total gas flow rate by about a factor of two resulted in an insignificant change in S retention ($\Delta < 10\%$).

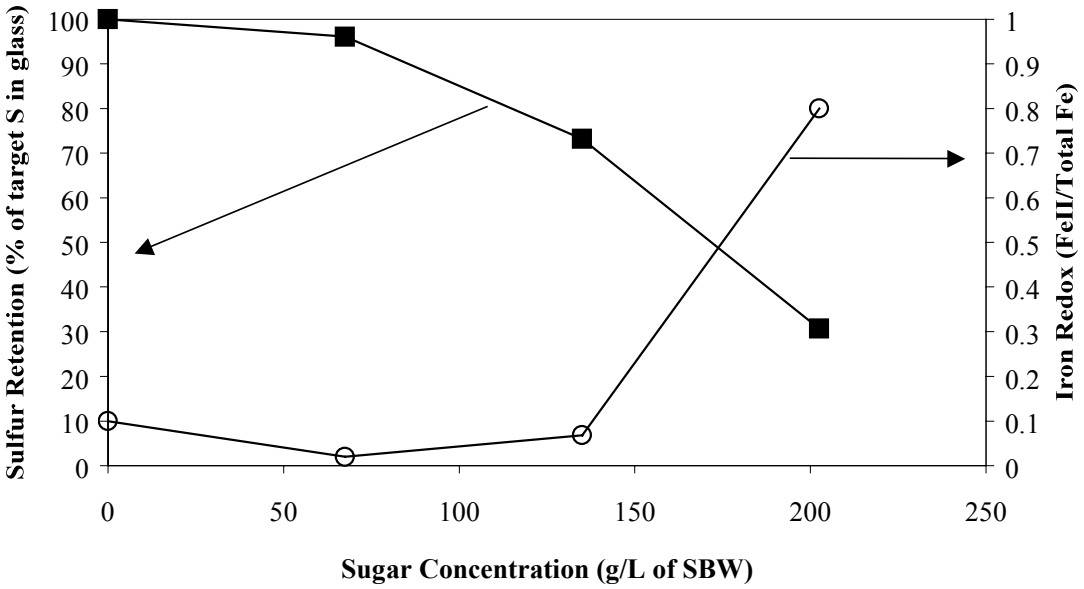


**Figure 4.2. Influence of the Sugar Concentration in the SBW Feed on the Retention of S and Iron Redox for Glasses Prepared Using the CSM**

These sweep-gas results are very much different than those obtained from the crucible tests, in which the glass S retention values were dramatically altered, 100% vs. 23% respectively, for experiments run with no sweep gas vs. those run with a 2300-ccm sweep gas (see Section 2.4.5). However, it should be noted that unlike in CSM runs (as well as RSM, EV-16, and even QC runs), where potentially no sweep gas could be employed and a significant batch-gas flow rate would still maintain mass transport out of the melt area, crucible runs with no sweep gas and a sealed lid would theoretically have no, or very little, mass transport out of the melt area. In other words, the effect of sweep/batch gas flow rate on the glass S retention might be considered nearly "digital." There is an enormous difference between no flow and a finite flow, but variations in the finite flow rate do not significantly influence the glass S retention values.

The concentration of sulfur species in the CSM off-gas scrubber solutions was also analyzed using several techniques. We chose to look at the mass balance for two runs: CSM42701 and CSM51401. These two runs have the sulfur concentration in both the glass and the scrubber solution analyzed by the same technique (ICP). This analysis is summarized in Table 4.4 and Table 4.5. Until we obtain resolution in the difference between the results obtained from different techniques, we cannot draw any firm conclusions about S partitioning during these or any of the other CSM runs.

Two typical examples of the GC-MS off-gas data obtained from CSM runs are included in Figure 4.3. $N_2O$ was generally very low in concentration and could not be quantitatively determined. The $SO_2$ responses were all very low—typically around 1 to 3 ppm. Those for the runs shown in Figure 4.3 are included in Figure 4.4.

**Table 4.4. Amount of S in Glasses and Scrubber Solutions for CSM Runs Based on the Amount of Feed Vitrified. ICP was used to determine the concentration of S in all cases.**

| Run | Notation | Volume of feed used (mL) | Target mass S in feed (g) | Mass S in scrub solution (g) | Mass S in glass (g) |
|---|---|---|---|---|---|
| CSM42701 | base run | 90.3 | 0.147 | 0.0386 | 0.108 |
| CSM51401 | fast feed | 93.8 | 0.153 | 0.0679 | 0.109 |

**Table 4.5. Partitioning of S Between Glass and Scrubber Solution for Two CSM Runs**

| | | S Partitioning, ICP Analysis (% of target S in feed) | | |
|---|---|---|---|---|
| Run | Notation | Glass | Scrub Solution | Sum |
| CSM42701 | base run | 73.2 | 26.2 | 99.4 |
| CSM51401 | fast feed | 71.1 | 44.4 | 115.5 |

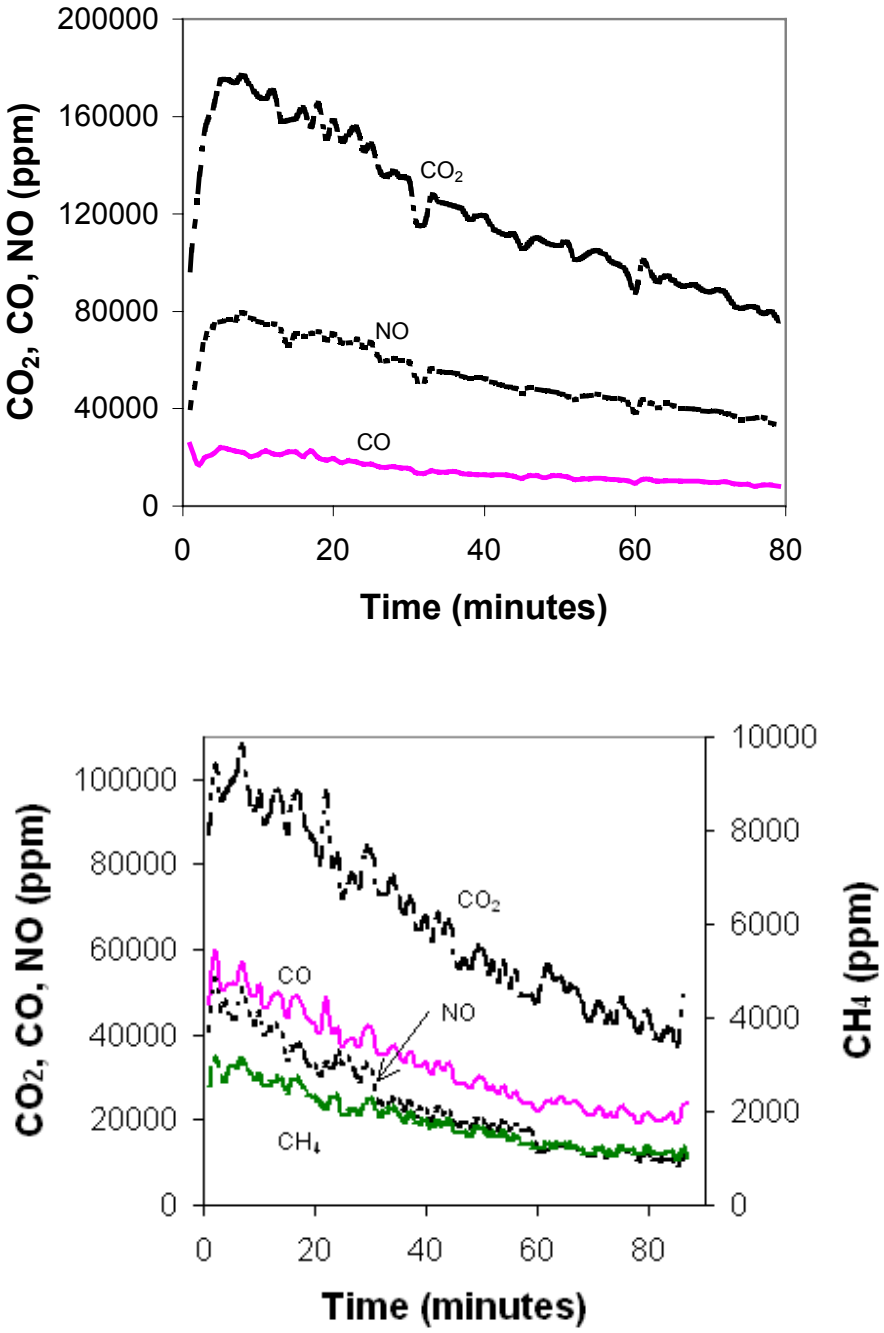


**Figure 4.3. GC-MS Responses Obtained from Two Typical CSM Runs. The upper plot (above) is from the glycolic acid run (CSM61201). The lower plot is from the high sugar run (CSM60801).**

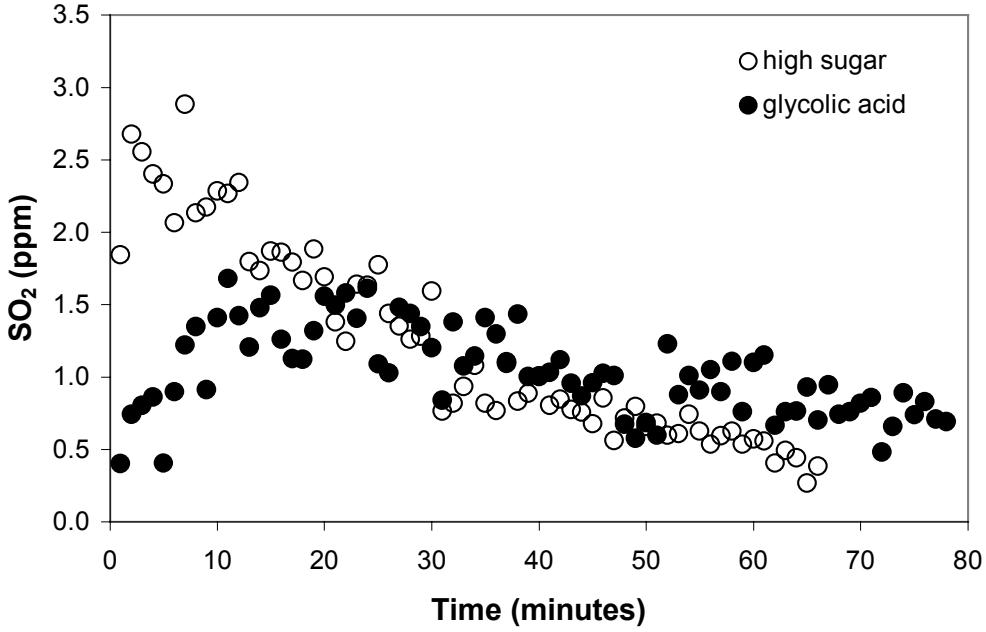


**Figure 4.4. GC-MS $SO_2$ Responses Obtained from CSM Runs CSM60801 (high sugar) and CSM61201 (glycolic acid)**

## 4.3 $SO_2$ Concentration in the Off Gas

On an oxide basis, there is 4.084 g $SO_3$ per liter of SBW-9 feed at 35 mass% waste loading. The typical feed rate into the CSM is 1.25 mL feed per minute, which corresponds to a rate of $SO_3$ feed of $5.1 \times 10^{-3}$ g/min. If all of this $SO_3$ is volatilized as $SO_2$(g), this would correspond to an $SO_2$ off-gas rate of $4.1 \times 10^{-3}$ g/min or $6.4 \times 10^{-5}$ moles/min.

A typical sweep-gas flow rate for a CSM run optimized for GC-MS analysis is 300 $cm^3$/min. However, we would expect a batch-gas production rate of 0.049 moles/min (≈1200 mL/min) at a feed rate of 1.25 mL/min. This is based on approximately 50% water collection (only about 50 mL of water was collected during CSM runs, whereas we would expect about 100 mL from the amount of feed used) and the thermodynamic modeling results presented earlier,

So, during 1 min of CSM operation at a feed rate of 1.25 mL/min and a sweep-gas flow of 1500 mL/min, assuming that all the S in the feed is volatilized as $SO_2$(g), we should expect $6.4 \times 10^{-5}$ moles $SO_2$ per $6.1 \times 10^{-2}$ moles sweep gas. This corresponds to a concentration of $SO_2$ in the off gas of about 1000 ppm. Based on the sulfur retention values obtained from the glasses prepared from a baseline CSM run, we know that only about 23% of the total sulfur is lost during the vitrification process. Thus, still assuming that all of the sulfur in the feed is volatilized as $SO_2$(g), we should expect at most 230 ppm $SO_2$ in the off gas being collected during the vitrification process.

As mentioned earlier, we do not know the fate of the $SO_2$ that might be generated during the vitrification process. There are a number of "sinks" for $SO_2$, both in large-scale melters and in the CSM

setup. Ideally, based on the difference between the sulfur between what goes into the CSM and what goes into the glass and scrubber, we should be able to place an upper limit on how much $SO_2$ might be reaching the GC-MS in the CSM setup. However, this would require more accurate S partitioning information. For example, we are obtaining greater than 100% mass balance in one of the two examples listed in Table 4.4 and Table 4.5 (CSM51401), which would tend to cast doubt about the validity of the other example in which the mass balance is less than 100% (CSM47201). Even if we believe the mass-balance results from the CSM42701 run, the data suggest that a maximum of only about 0.6% of the total sulfur could be evolved as $SO_2$. This is in dramatic contrast with the results obtained from the RSM runs in which it was estimated that approximately 15 to 25% of the total sulfur could be evolved as $SO_2$ (see Section 3.2). Until we can account for these problems and obtain a resolution in the difference between the results obtained from different techniques, we cannot estimate, for example, how much $SO_2$ might be generated.

To get an initial idea about how much $SO_2$ we might be able to detect in the CSM setup, we deliberately added $SO_2$-containing gas through the sweep-gas line during two baseline runs (CSM62101 and CSM62701) to concentrations of up to ≈90 ppm (i.e., 40% of the maximum value we would expect during a baseline run). No change in the $SO_2$ GC-MS response was noted during these $SO_2$ injections. A substantial increase in possible $SO_2$ concentration cannot be observed using the CSM set up, presumably due to the trapping of the $SO_2$ in the aforementioned sinks. Thus, even if $SO_2$ is being generated, these results indicate that a significant amount of it would get trapped in the CSM before even getting to the GC-MS, making its detection even more difficult.

Although the CSM could not provide definitive results in terms of determining the $SO_2(g)$ concentration in the off gas, we did demonstrate its usefulness in studying the vitrification of liquid waste streams on a laboratory scale, as will be discussed in Section 5.

# 5.0 Practical Implications and Ongoing Work

We developed a CSM to study the effects of feed chemistry and process parameters. Using the CSM, we can continuously feed aqueous SBW feed directly into a crucible at melt temperature. Table 5.1 summarizes some of the S-retention results obtained from pertinent CSM runs and compares them to the results obtained from larger scale continuous melters (RSM and EV-16) as well as those from batch crucible melts.

Although sealed crucible studies (which are the typical experiments that have been run to date for such work) are useful screening tools to select between different melter-feed chemistries, they do not provide the required variation in process (and in some cases, feed chemistry) needed to address issues pertaining to the vitrification of complex aqueous wastes, such as SBW. Larger scale melts are time consuming and costly.

A review of the work presented in this report indicates that there are numerous variables influencing the S retention in glass that need to be considered: additive mix composition (e.g., SBW-4 vs. SBW-9), waste loading, type and amount of reductant, feed rate, type of feed (i.e., dried feed vs. aqueous feed), type of melter, sweep-gas rate, acid and sulfate concentration in the feed, and even how the glass samples were characterized (i.e., XRF vs. ICP). This latter point is a critical issue that has arisen during the preparation of this report, and it is a priority for ongoing work.

Ideally, the CSM setup will allow researchers to alter feed chemistry and representative processing parameters quickly and efficiently while providing the same results obtained from larger scale melters. To do this, we must first demonstrate this latter aspect: in this case, that the results obtained from the CSM can duplicate those obtained from the RSM or EV-16 melters. In most cases, though, we cannot make direct comparisons between from the CSM and RSM or EV-16 runs because too many variables are being changed. Based on the initial results presented here, however, we can make some estimates as will be discussed next.

We have already demonstrated that the effect of waste loading, sweep-gas rate, and acid concentration in the feed on the S retention in the final glass is insignificant based on these initial results. Thus, these variables can be ignored for the moment. Of the variables that remain, we have a rudimentary understanding of what the effect of changing some of these variables within a certain range has on the S retention in the final glass. Table 5.1 compares those melting experiments from among the crucible, RSM, CSM, and EV-16 runs whose process and chemistry variations fall into this latter category and whose glass S retention values were determined by ICP.

For example, the only major difference between experiments 1 and 2 in Table 5.1 is the additive mix. Using the observed difference in glass S retention between SBW-4 and SBW-9 additive mixes (78% vs. 102%, respectively) allows us to normalize the glass S retention value for Experiment 3 in Table 5.1 (the QC run using SBW-4 additive mix), as well as Experiment 1, with respect to the SBW-9 additive mix. Likewise, we know the effect of sugar content on the S retention in the final glass (see Figure 4.2). So we can estimate the glass S retention value of Experiments 1, 3, and 6 in Table 5.1 based on 135 g/L sugar as opposed to 141 g/L or 160 g/L. Table 5.1 lists the normalized S-retention values based on a feed consisting of a SBW-9 additive mix and 135 g of sugar per liter of simulated waste.

For those experiments that use an aqueous feed, from Table 5.1 one notes essentially two normalized feed rates: Experiments 5 and 6 use a feed rate of 6 to 7 mL/cm$^2$-h, while experiments 4, 7, 8, and 9 use a feed rate of about 12 to 16 mL/cm$^2$-h. We can estimate the glass S-retention values based on a single feed-rate group. This assumes that the former group can be represented by a feed rate of 6 mL/cm$^2$-h, along with its accompanying glass S retention value of 93%, and the latter by a feed rate of 15 mL/cm$^2$-h, along with its S retention value of 73%.

Based on chemical analyses made using the same technique (ICP) and the normalized data presented in Table 5.1, several preliminary results are suggested. First, the crucible experiments (both with and without sweep gas) using dried SBW feed do not compare very well with any of the liquid fed experiments, even if we have underestimated the amount of experimental error. Perhaps adjustment of the sweep gas flow rate might allow us to bring the crucible results in line with the liquid-fed melter results, but certainly additional experiments will need to be performed to get the required data. This is an area we will want to pursue further.

Secondly, we determined that the CSM is a good screening tool that produces S-partitioning results that match reasonably well to the results obtained from the larger scale melter EV-16 (-2001-1), yet allows for numerous process and feed chemistry variables to be investigated relatively quickly and easily. The CSM results are significantly different (>10% Δ') from the RSM runs, but it should be noted that the RSM results themselves are significantly different from the EV-16 (-2001-1) results. We are still uncertain why there is a significant difference between the EV-16 (-2001-1) run and the RSM runs. One reason could be the differences in melter design (e.g., melt depth, melt surface area, shape of melter, etc.). These issues will continue to be investigated in ongoing work.

Having demonstrated that the CSM setup can yield results similar to those obtained from larger liquid-fed melters, we can use the CSM results to help us better understand the vitrification of SBW. For the CSM experiments performed to date, we have identified several process and feed-chemistry variables that may influence the degree of salt formation and S retention in the glass product. These include feed rate as well as the concentration of sulfate, sugar (and perhaps other reductants), and $HNO_3$ in the feed.

A high feed rate significantly increases the tendency for salt formation as well as moderately decreases the amount of S retained in the final glass product (presumably because S that would ordinarily be in the glass is segregating into a molten salt layer). Slow feed rates tend to increase the incorporation of S in the final glass.

An increase in the concentration of sulfate in the feed slightly increases the degree of salt coverage on the melt surface. There is also considerably more S (based on the amount of S in the feed) lost (likely to the off gas).

**Table 5.1. Comparison of the S Retention Results Obtained from Various Melting Experiments**

| | | | | | | S retention | | |
|---|---|---|---|---|---|---|---|---|
| **Exp.** | **Additive Mix** | **Waste loading and reductant** | **Experimental set up or run** | **Normalized feed rate ($mL/cm^2$-h)** | **Mass% $SO_3$ in Glass (by ICP)** | **Measured (% of target S in glass)** | **Normalized[(a)] (% of target S in glass)** | **Δ' (%)[(b)]** |
| 1 | SBW-4 | 35%, 141 g/L sugar | crucible | dried feed | 0.98 | 78 | 100 | +39 |
| 2 | SBW-9 | 32%, 135 g/L sugar | crucible | dried feed | 1.10 | 102 | 100 | +39 |
| 3 | SBW-4 | 35%, 141 g/L sugar | QC | dried feed | 0.80 | 64 | 84 | +17 |
| 4 | SBW-9 | 32%, 135 g/L sugar | CSM, 42701 | 15.0 | 0.84 | 73 | 73 | +1 |
| 5 | SBW-9 | 32%, 135 g/L sugar | CSM, 60101 | 6.0 | 1.06 | 93 | 73 | +1 |
| 6 | SBW-9 | 30%, 160 g/L sugar | EV-16-2001-1 | 7.0 | 0.77 | 72 | 72 | 0 |
| 7 | SBW-9 | 30%, 135 g/L sugar | RSM-01-1, A-B | 12.1 | 0.68 | 63 | 63 | -12 |
| 8 | SBW-9 | 32%, 135 g/L sugar | RSM-01-1, C-D | 15.9 | 0.66 | 56 | 56 | -22 |
| 9 | SBW-9 | 35%, 135 g/L sugar | RSM-01-1, E | 13.7 | 0.70 | 56 | 56 | -22 |
| 10 | SBW9 | 335%, 135 g/L sugar | crucible w/purge | dried feed | 0.27 | 24 | 24 | -67 |

(a) Normalized % of target S in glass is based on an SBW-9 additive mix, 135 g sugar per liter of simulated waste, and, for aqueous feeds, a normalized feed rate of 15 $mL/cm^2$-h.

(b) Δ', in %, compares the normalized S retention value for a given experiment to that of the EV-16-2001-1 experiment and is equal to 100x(normalized S retention—72)/72.

Increasing the concentration of sugar, $HNO_3$, or both greatly diminishes the degree of salt coverage on the melt surface. The concentration of sugar in the feed dramatically influences the amount of S retained in the glass product.

Additional CSM experiments involving a more refined variation of these process and feed-chemistry parameters will be performed in ongoing research. Furthermore, new parameters, especially the effect of additive composition, will be investigated.

Finally, as additional analytical data are received from the CSM experiments already performed and discussed here, and when we clarify the differences in results obtained by different analytical techniques, we will be able to provide further information concerning S partitioning between glass, molten salt, and off gas.

# 6.0 References


Abe, O., T. Utsunomiya, and Y. Hoshino. 1983. "The Reaction of Sodium Nitrate with Silica," *Bull. Chem. Soc*. Japan **56**, 428–433.

Beitel, G. A. 1976. *Sodium Nitrate Combustion Limit Tests.* ARH-LD-123, Informal Report, Atlantic Richfield Hanford Company, Richland, Washington.

Bray, L. A. 1963. *Denitration of PUREX Wastes with Sugar*. HW-76973, Hanford Atomic Products Operation, Richland, Washington.

Cotton, F. A., and G. Wilkinson. 1980a. *Advanced Inorganic Chemistry*, Fourth Edition, John Wiley and Sons, New York.

Cotton, F. A. and G. Wilkinson. 1980b. *Advanced Inorganic Chemistry*, Fourth Edition, John Wiley and Sons, New York.

Darab, J. G., E. M. Meiers, and P. A. Smith. 1999. "Behavior of Simulate Hanford Slurries During Conversion to Glass," In *Mat. Res. Soc. Symp. Proc.*, Vol. 556, Materials Research Society, Warrendale, Pennsylvania, pp. 215–222.

Darab J.G. and P.A. Smith. 1996. "Chemistry of Technetium and Rhenium Species during Low-Level Radioactive Waste Vitrification," *Chem. Mater*. **8**, 1004–1021.

Goles R. W., J. M. Perez, B. D. MacIsaac, D. D. Siemer, and J. A. McCray. 2001. *Testing Summary Report INEEL Sodium Bearing Waste Vitrification Demonstration RSM-01-1*, PNNL-13522, Pacific Northwest National Laboratory, Richland, Washington.

Matson, D. W., J. G. Darab, T. D. Brewer, and P. D. Kaviratna. 1998. "Production of Nanocrystalline Sulfated Zirconia Catalysts via a Flow-through Hydrothermal Process," In *Mat. Res. Soc. Proc.* Vol. 520, Materials Research Society, Warrendale, Pennsylvania, pp. 287–292.

Musick, C. A., B. A. Scholes, R. D. Tillotson, D. M. Bennert, J. D. Vienna, J. V. Crum, D. K. Peeler, I. A. Reamer, D. F. Bickford, J. C. Marra, N. L. Waldo. 2000. *Technical Status Report: Vitrification Technology Development Using INEEL Run 78 Pilot Plant Calcine*, INEEL\EXT-2000-00110. Idaho National Engineering and Environmental Laboratory, Idaho Falls, Idaho.

Peeler, D. K., J. D. Vienna, T. B. Edwards, J. V. Crum, I.A. Reamer, M. J. Schweiger, and R. J. Workman. 2001. *Glass Formulation development for INEEL Sodium-Bearing Waste (WM-180)*, WSRC-TR-2001-00295, Rev. 0, Westinghouse Savannah River Company, Aiken, South Carolina.

Pegg I. L., H. Gan, I. S. Muller, D. A. McKeown, and K. S. Matlack. 2001. *Summary of Preliminary Results on Enhanced Sulfate Incorporation During Vitrification of LAW Feeds*, VSL-00R3630-1, Vitreous State Laboratory, The Catholic University of America, Washington, DC 20064.

Smith, P. A., J. D. Vienna, and P. Hrma. 1995. "The Effect of Melting Reactions on Laboratory-Scale Waste Vitrification," *J. Mater. Res.* **10**, 2137–2149.

Smith, H. D., E. O. Jones, A. J. Schmidt, A. H. Zacher, M. D. Brown, M. R. Elmore, and S. R. Gano. 1999. *Denitration of High Nitrate Salts Using Reductants*, PNNL-12144, Pacific Northwest National Laboratory, Richland, Washington.

U.S. Department of Energy (DOE). 1995. *The INEEL Spent Nuclear and Environmental Restoration and Waste Management Programs Environmental Impact Statement,* DOE\EIS-0202-F, Washington, D.C.

Vienna, J. D., M. J. Schweiger, D. E. Smith, H. D. Smith, J. V. Crum, D. K. Peeler, I. A. Reamer, C. A. Musick, and R. D. Tillotson. 1999. *Glass Formulation Development for INEEL Sodium-Bearing Waste*, PNNL-12234, Pacific Northwest National Laboratory, Richland, Washington.

# Distribution

**No. of Copies**

**OFFSITE**

1 DOE Idaho Operations Office
750 DOE Place, MSIN: 1145
Idaho Falls, ID 83402
Attn: Kieth Lockie

10 Idaho National Engineering and Environmental Laboratory
P. O. Box 1625
Idaho Falls, ID 83415

| | | |
|---|---|---|
| Attn: | R. R. Kimmitt | MS 5218 |
| | C. A. Musick (5) | MS 5218 |
| | A. L. Olson | MS 5218 |
| | K. J. Perry | MS 5218 |
| | J. Rindfleisch | MS 5218 |
| | B. A. Scholes | MS 5218 |

10 Westinghouse Savannah River Co.
SRTC, Bldg 773-A
Aiken, South Carolina 29808

| | | |
|---|---|---|
| Attn: | D. F. Bickford | 773-43A |
| | E. W. Holtzscheiter | 773-A |
| | J. George | 773-43A |
| | S. L. Marra | 704-1T |
| | D. K. Peeler (5) | 773-43A |
| | D. Witt | 704-1T |

**No. of Copies**

**ONSITE**

1 CH2M Hill Hanford Group

| | |
|---|---|
| J. O. Honeyman | R2-58 |

1 DOE Richland Operations Office

| | |
|---|---|
| T. P. Pietrok | K8-50 |

2 DOE Office of River Protection

| | |
|---|---|
| R. Carreon | H6-60 |
| J. E. Cruz | H6-60 |

1 Numatec Hanford Company

| | |
|---|---|
| S. L. Lambert | R3-75 |

29 Pacific Northwest National Laboratory

| | |
|---|---|
| T. M. Brouns | K9-69 |
| W. F. Bonner | K9-14 |
| J. V. Crum | K6-24 |
| J. G. Darab (5) | K3-59 |
| P. Hrma | K6-24 |
| R. Goles | K6-24 |
| D. Graham | K6-24 |
| D. S. Kim | K6-24 |
| E. V. Morrey | P7-28 |
| L. M. Peurrung | K6-24 |
| J. D. Vienna (5) | K6-24 |
| B. J. Williams (TFA) (8) | K9-69 |
| Technical Report Files (2) | P8-55 |

2 Washington Group

| | |
|---|---|
| J. R. Harbour | H4-02 |
| J. M. Perez | H4-02 |